

Localized wave solutions and rogue wave solutions for the complex modified KdV equation under the elliptic function background

Xin-Yi Xu(许馨苡), Huan-He Dong(董焕河)

Citation: Chin. Phys. B. 35, 090204 (2026). DOI: 10.1088/1674-1056/ae7277 | CSTR: 32038.14.CPB.ae7277
http://cpb.iphy.ac.cn; http://iopscience.iop.org/cpb

What follows is a list of articles you may be interested in

High-order doubly localized waves in (2+1)-dimensional Maccari system

Xue-Wei Yan(严学威), Jin-Jin Mao(茆晋晋), Min-Jie Dong(董敏杰)
Chin. Phys. B. 35, 070201 (2026). DOI: 10.1088/1674-1056/ae0682 | CSTR: 32038.14.CPB.ae0682

Dynamical analysis and localized waves of the n-component nonlinear Schrödinger equation with higher-order effects

Yu Lou(娄瑜), Guoan Xu(许国安)
Chin. Phys. B. 34, 030201 (2025). DOI: 10.1088/1674-1056/ada435 | CSTR: 32038.14.CPB.ada435

Anomalous diffusion in branched elliptical structure

Kheder Suleiman, Xuelan Zhang(张雪岚), Erhui Wang(王二辉), Shengna Liu(刘圣娜), Liancun Zheng(郑连存)
Chin. Phys. B. 32, 010202 (2023). DOI: 10.1088/1674-1056/ac5c39

Exact solutions of a (2+1)-dimensional extended shallow water wave equation

Feng Yuan(袁丰), Jing-Song He(贺劲松), Yi Cheng(程艺)
Chin. Phys. B. 28, 100202 (2019). DOI: 10.1088/1674-1056/ab3e65

Truncated series solutions to the (2+1)-dimensional perturbed Boussinesq equation by using the approximate symmetry method

Xiao-Yu Jiao(焦小玉)
Chin. Phys. B. 27, 100202 (2018). DOI: 10.1088/1674-1056/27/10/100202

SPECIAL TOPIC — Nonlinear localized waves: Theory, methods and applications

Localized wave solutions and rogue wave solutions for the complex modified KdV equation under the elliptic function background

Xin-Yi Xu(许馨苡) and Huan-He Dong(董焕河)†

College of Mathematics and Systems Science, Shandong University of Science and Technology, Qingdao 266590, *China*

(Received 1 April 2026; revised manuscript received 20 May 2026; accepted manuscript online 26 May 2026)

Nonlinear wave phenomena frequently evolve on periodically fluctuating backgrounds, yet systematic theoretical frameworks for the complex modified Korteweg–de Vries (cmKdV) equation on elliptic backgrounds remain incomplete. To address this, this study systematically investigates localized and rogue wave solutions of the cmKdV equation on elliptic function backgrounds. The methodology combines the Theta function representation with the Darboux transformation within a genus-1 algebraic geometry framework. By utilizing linear combinations of Lax pair solutions and small-parameter expansions near the branch points of the spectral curve, the study extracts degenerate vector solutions. The results explicitly present five typical localized waves, including elliptic solitons and elliptic breathers, on both cn-type and dn-type backgrounds. Furthermore, general formulas for higher-order rogue waves are derived. The work reveals distinct dynamic behaviors, such as the coexistence of different families of rogue waves on cn-type backgrounds and nonlinear superpositions on modulationally stable dn-type backgrounds.

Keywords: cmKdV equation, elliptic function, localized wave, rogue wave

PACS: 02.30.Ik, 05.45.Yv, 05.45.–a, 02.60.Cb

DOI: 10.1088/1674-1056/ae7277 **CSTR:** 32038.14.CPB.ae7277

1. Introduction

Nonlinear wave phenomena pervade a wide range of physical systems, from optical fiber communications and plasma physics to fluid mechanics and atmospheric dynamics. In contrast to linear systems, where waves superpose trivially, the interplay among waves in nonlinear media gives rise to rich dynamical behaviors — energy localization, self-focusing, and modulational instability — that remain central topics in modern physics and applied mathematics. Among the most remarkable manifestations of nonlinearity is the soliton, a localized wave packet that preserves its shape and velocity through collisions. The particle-like nature of solitary waves was first identified by Zabusky and Kruskal[1] in numerical simulations of the Korteweg–de Vries (KdV) equation, triggering more than half a century of developments in soliton theory. Shortly afterwards, Gardner *et al.*[2] introduced the inverse scattering transform (IST), providing an exact framework for solving the KdV initial-value problem. Lax[3] subsequently formulated the operator-pair (Lax pair) approach that links nonlinear evolution equations with linear spectral problems, establishing a unified criterion for integrability. In recent years, data-driven approaches such as physics-informed neural networks have also been employed to investigate nonlinear wave dynamics in geophysical fluids.[4] The IST was extended to the nonlinear Schrödinger (NLS) equation by Zakharov and Shabat,[5] and Ablowitz *et al.*[6,7] constructed the general AKNS hierarchy, which encompasses the KdV, modified Korteweg–de Vries (mKdV), NLS, and sine-Gordon equations within a single integrable framework.

Within the KdV hierarchy, the complex modified Korteweg–de Vries (cmKdV) equation

$$\psi_t + \psi_{xxx} + 6|\psi|^2\psi_x = 0 \tag{1}$$

is a class of integrable models with significant theoretical and applied value. The real-valued mKdV equation was first introduced and solved via the IST by Wadati.[8,9] As its natural generalization to the complex domain, the cmKdV equation has important applications in nonlinear optics. When an optical pulse is compressed to contain only a few oscillation cycles, the slowly varying envelope approximation fails, and the cmKdV equation provides an appropriate description of circularly polarized few-cycle pulse propagation in Kerr media. Leblond, Triki *et al.*[10] derived this model rigorously from Maxwell's equations and subsequently delineated the applicable regimes of various few-cycle evolution equations.[11,12] He *et al.*[13] investigated rogue wave solutions of the cmKdV equation on plane-wave backgrounds using the Darboux transformation, thereby elucidating the role of this equation in characterizing few-cycle optical rogue waves. Lan[14] further constructed multi-soliton, breather-like, and bound-state soliton solutions of the cmKdV equation in the context of optical fibers, enriching the understanding of localized wave

†Corresponding author. E-mail: donghuanhe@126.com

© 2026 Chinese Physical Society and IOP Publishing Ltd. All rights, including for text and data mining, AI training, and similar technologies, are reserved.

structures for this model. Beyond optics, the cmKdV equation also finds application in analyzing nonlinear vector waves in molecular chains.[15] From the standpoint of mathematical structure, the cmKdV equation possesses hallmarks of complete integrability, including a Lax pair, infinitely many conserved quantities,[16] and a bi-Hamiltonian structure.[17]

In parallel with the deepening understanding of integrable structures, a powerful arsenal of solution-construction methods has been developed. Hirota's bilinear method[18,19] offers a direct algebraic route to multi-soliton solutions. The Darboux transformation was systematically established by Matveev and Salle,[20] and further developed by Gu *et al.*[21] Additional techniques — including the Bäcklund transformation[22] and the Riemann–Hilbert method[23] — have been refined and consolidated into the standard toolkit of integrable systems theory.[24,25] A particularly influential recent advance is the generalized Darboux transformation proposed by Guo *et al.*[26] for the NLS equation, which enables the extraction of higher-order rogue wave solutions through Taylor expansions at degenerate spectral points. This technique has since been extended to numerous integrable models, including the derivative NLS equation[27,28] and the Hirota equation.[29] He *et al.*[30] further elucidated the generation mechanism of higher-order rogue waves, and Yang[31] provided a comprehensive account of both bilinear and Darboux-transformation approaches to rogue waves. For the mKdV equation specifically, Wadati and Ohkuma[32] studied multipole solutions; Tsuchida and Wadati[33] investigated the integrability of coupled mKdV systems; Alejo and Muñoz[34] proved the nonlinear stability of mKdV breathers and analyzed the dynamics of cmKdV solitons and their implications for breather stability.[35]

Traditional soliton theory has been largely confined to zero or constant backgrounds. In realistic physical settings, however, nonlinear waves frequently evolve on periodically modulated backgrounds — continuous-wave carriers in optical fibers, regular wave trains in the ocean, or periodic plasma oscillations. Mathematically, the most general periodic traveling-wave solutions of integrable equations are expressed via Jacobi elliptic functions, rooted in the finite-band integration theory.[36,37] Belokolos *et al.*[38] comprehensively surveyed the application of algebro-geometric methods to nonlinear integrable equations, while Cao *et al.*[39] established connections between the KP equation and finite-dimensional integrable systems through confocal involutive representations. Superimposing localized structures on elliptic function backgrounds not only reveals the rich dynamics of nonlinear waves in periodic media but also maintains deep intrinsic connections with the phenomenon of modulational instability.[40–42]

For the focusing NLS equation, substantial progress has been achieved in constructing exact solutions on periodic backgrounds. Chen and Pelinovsky[40] employed the Darboux transformation to obtain rogue wave solutions on dn-type and cn-type periodic-wave backgrounds and determined the rogue-wave amplification factors as functions of the elliptic modulus. Subsequently, they generalized the method to double-periodic backgrounds,[43] uncovering multiple rogue-wave families associated with distinct branch points. On periodic standing-wave backgrounds, they systematically constructed rogue waves and analyzed their connection to modulational instability.[44] Grinevich and Santini[45] provided an exact analytical description of rogue wave recurrence in the periodic NLS Cauchy problem via the finite-gap method. Bertola *et al.*[46] investigated rogue waves in multiphase NLS solutions, and Bertola and Tovbis[47] established exact upper bounds for the maximum amplitude of finite-band solutions. Feng *et al.*[48] constructed multi-breather and higher-order rogue wave solutions on elliptic backgrounds for the NLS equation, furnishing unified determinant-form formulas.

Turning to the mKdV equation, Chen and Pelinovsky[49] pioneered the study of rogue waves on periodic traveling-wave backgrounds, demonstrating that dn-type periodic waves are modulationally unstable whereas cn-type periodic waves are modulationally stable. In subsequent work,[50] they provided a complete classification of the most general periodic traveling-wave solutions and systematically constructed rogue waves on these backgrounds. Ling and Sun[51] carried out a rigorous spectral stability analysis of elliptic function solutions for the real mKdV equation, establishing stability conditions under subharmonic perturbations via the squared-eigenfunction method. Building on this foundation, they constructed multi-elliptic-localized wave solutions[52] with unified analytical expressions using the Darboux–Bäcklund transformation and Jacobi Theta functions, and proved the elastic nature of collisions. More recently, Ling and Sun[41] established a quantitative correspondence between elliptic rogue waves and modulational instability.

Despite these advances, the study of the cmKdV equation on elliptic function backgrounds remains unsystematic and incomplete. Sinthuja *et al.*[53] used the Darboux transformation to investigate rogue waves on elliptic backgrounds, but their results were confined to special first-order examples without providing general higher-order formulas. Rao *et al.*[54] studied multi-soliton and multi-breather solutions on periodic cmKdV backgrounds via the bilinear method. Hu and Gegen[55] recently constructed N-breather solutions as well as hybrid rogue-wave–breather solutions for the cmKdV equation, providing further insight into the coexistence of breather and rogue wave structures. To date, however, a unified theoretical framework encompassing general localized wave formulas and systematic rogue wave expressions for the cmKdV equation on elliptic backgrounds has not been established.

The present work aims to fill this gap. By combining Theta function representations within the genus-1 algebro-geometric framework with both the standard and generalized Darboux transformations, we systematically construct localized wave solutions and rogue wave solutions of the cmKdV equation on elliptic function backgrounds. Complete Theta function representations for the elliptic periodic solutions and the fundamental Lax pair solutions are first derived. Utilizing linear combinations of the Lax pair vector solutions together with Theta function addition formulas, we obtain explicit determinant formulas for n-fold localized wave solutions on both cn-type and dn-type backgrounds, encompassing elliptic solitons, elliptic breathers, elliptic two-solitons, elliptic soliton-breathers, and elliptic two-breathers. Through small-parameter expansions near the branch points of the spectral curve and the generalized Darboux transformation, general determinant formulas for n-th order rogue waves are derived. On the cn-type background, two identical rogue wave families arise from the involution symmetry of the Lax pair, while on the modulationally stable dn-type background, the two branch points generate distinct elliptic-soliton and elliptic-breather modes that combine into elliptic-soliton-breathers at second order.

2. Theta function representations of elliptic function solutions and Lax pair solutions

In this section, we first derive the elliptic function solutions of the cmKdV equation and then obtain the corresponding solutions of the Lax pair using algebraic geometry methods, which are detailed in monographs. Here we only consider the genus-1 case, where the solutions can be represented using elliptic functions and integrals.

This paper primarily investigates the focusing cmKdV equation, whose Lax pair can be written as follows:

$$\begin{aligned}&\Phi_x = \boldsymbol{M}\Phi, \quad \boldsymbol{M} = -\mathrm{i}\lambda\sigma_3 + \boldsymbol{Q},\\ &\Phi_t = \boldsymbol{N}\Phi, \quad \boldsymbol{N} = \begin{bmatrix} A & B \\ C & -A \end{bmatrix},\end{aligned} \tag{2}$$

where

$$\begin{aligned}&\sigma_3 = \begin{bmatrix} 1 & 0 \\ 0 & -1 \end{bmatrix}, \quad \boldsymbol{Q} = \begin{bmatrix} 0 & \psi \\ -\psi^* & 0 \end{bmatrix},\\ &A = -4\mathrm{i}\lambda^3 + 2\mathrm{i}\lambda|\psi|^2 + \psi_x^*\psi - \psi_x\psi^*,\\ &B = 4\lambda^2\psi + 2\mathrm{i}\lambda\psi_x - \psi_{xx} - 2|\psi|^2\psi,\\ &C = -4\lambda^2\psi^* + 2\mathrm{i}\lambda\psi_x^* - \psi_{xx}^* - 2|\psi|^2\psi^*.\end{aligned} \tag{3}$$

By applying the compatibility condition $\Phi_{xt} = \Phi_{tx}$ or the zero-curvature equation $\boldsymbol{M}_t - \boldsymbol{N}_x + [\boldsymbol{M}, \boldsymbol{N}] = 0$, we can recover the cmKdV equation. The potential functions $\boldsymbol{M}$ and $\boldsymbol{N}$ satisfy the symmetry relations $\boldsymbol{M}^\dagger(\boldsymbol{Q};\lambda^*) = -\boldsymbol{M}(\boldsymbol{Q};\lambda)$ and $\boldsymbol{N}^\dagger(\boldsymbol{Q};\lambda^*) = -\boldsymbol{N}(\boldsymbol{Q};\lambda)$, where the symbol † denotes the Hermitian conjugate. Based on the above symmetry, if $\Phi(x,t;\lambda)$ is a matrix solution to the Lax pair (2), then $\Phi^\dagger(x,t;\lambda^*)$ is a matrix solution to the adjoint Lax pair, which takes the following form:

$$\Psi_x = -\boldsymbol{M}(\boldsymbol{Q};\lambda)\Psi, \quad \Psi_t = -\boldsymbol{N}(\boldsymbol{Q};\lambda)\Psi. \tag{4}$$

As a more general symmetry, if $\Phi(x,t;\lambda)$ satisfies the Lax pair (2), then $(\mathrm{i}\sigma_2)\Phi^{\mathrm{T}}(x,t;-\lambda)(-\mathrm{i}\sigma_2)$ satisfies the adjoint Lax pair (4), where σ_2 is the Pauli matrix

$$\sigma_2 = \begin{pmatrix} 0 & -\mathrm{i} \\ \mathrm{i} & 0 \end{pmatrix}.$$

Based on the Lax pairs (2) and (4), we define a new matrix function

$$\boldsymbol{D}(x,t;\lambda) = -\frac{1}{2}\Phi(x,t;\lambda)\,(\mathrm{i}\sigma_2)\,\Phi^{\mathrm{T}}(x,t;-\lambda)\,(-\mathrm{i}\sigma_2).$$

It satisfies the following stationary zero-curvature equations

$$\boldsymbol{D}_x = [\boldsymbol{M}, \boldsymbol{D}], \quad \boldsymbol{D}_t = [\boldsymbol{N}, \boldsymbol{D}]. \tag{5}$$

The compatibility condition of the aforementioned stationary zero-curvature equations is given, and through the compatibility condition of the Lax pair and the Jacobi identity, the cmKdV equation can also be derived.

2.1. Elliptic function solutions

To obtain the analytical formula for the matrix function $\boldsymbol{D}(x,t;\lambda)$, we rewrite the matrix functions $\Phi(x,t;\lambda)$ and $\boldsymbol{D}(x,t;\lambda)$ according to the Lax pair (2) and the stationary zero-curvature Eqs. (5)

$$\begin{aligned}&\Phi(x,t;\lambda) = \begin{pmatrix} \phi_1(x,t;\lambda) & \phi_2(x,t;\lambda) \\ \varphi_1(x,t;\lambda) & \varphi_2(x,t;\lambda) \end{pmatrix},\\ &\boldsymbol{D}(x,t;\lambda) = \begin{pmatrix} -\mathrm{i}q(x,t;\lambda) & w(x,t;\lambda) \\ m(x,t;\lambda) & \mathrm{i}q(x,t;\lambda) \end{pmatrix},\end{aligned} \tag{6}$$

where

$$\begin{aligned}&q(x,t;\lambda) = \frac{\mathrm{i}}{2}\big(\phi_1(x,t;\lambda)\varphi_2(x,t;\lambda) - \phi_2(x,t;\lambda)\varphi_1(x,t;\lambda)\big),\\ &w(x,t;\lambda) = \phi_1(x,t;\lambda)\phi_2(x,t;\lambda),\\ &m(x,t;\lambda) = -\varphi_1(x,t;\lambda)\varphi_2(x,t;\lambda).\end{aligned} \tag{7}$$

$[\phi_i, \varphi_i]^{\mathrm{T}}$ $(i = 1,2)$ are two vector solutions to the Lax pair (2), and then we write out the stationary zero-curvature equations in more detail

$$\begin{aligned}&q_x = \psi^* w - \psi m, \quad w_x = -2\psi q - 2\mathrm{i}\lambda w,\\ &m_x = 2\psi^* q + 2\mathrm{i}\lambda m, \quad q_t = \mathrm{i}(Cw - Bm),\\ &w_t = 2Aw + 2\mathrm{i}Bq, \quad m_t = -2Am - 2\mathrm{i}Cq,\end{aligned} \tag{8}$$

where A, B, and C are given by Eq. (3).

For the genus-1 case, we assume that the matrix function $\boldsymbol{D}$ is a quadratic polynomial in λ

$$\boldsymbol{D} = \boldsymbol{D}_0(x,t)\lambda^2 + \boldsymbol{D}_1(x,t)\lambda + \boldsymbol{D}_2(x,t). \tag{9}$$

Substituting Eq. (9) into Eq. (5) and comparing the coefficients of λ, we obtain:

For the x-equation

$$\begin{aligned}
&\lambda^3 : \sigma_3 \boldsymbol{D}_0^{\text{off}} = 0,\\
&\lambda^2 : \boldsymbol{D}_{0,x} + 2\mathrm{i}\sigma_3 \boldsymbol{D}_1^{\text{off}} + [\boldsymbol{Q}, \boldsymbol{D}_0] = 0,\\
&\lambda^1 : \boldsymbol{D}_{1,x} + 2\mathrm{i}\sigma_3 \boldsymbol{D}_2^{\text{off}} + [\boldsymbol{Q}, \boldsymbol{D}_1] = 0,\\
&\lambda^0 : \boldsymbol{D}_{2,x} + [\boldsymbol{Q}, \boldsymbol{D}_2] = 0.
\end{aligned}$$

From this, we obtain

$$\begin{aligned}
\boldsymbol{D}(x,t;\lambda) \;=\; &-\mathrm{i}\alpha_0\sigma_3\lambda^2 + (-\mathrm{i}\alpha_1\sigma_3 + \mathrm{i}\alpha_0\boldsymbol{Q})\lambda - \mathrm{i}\alpha_2\sigma_3\\
&+\mathrm{i}\alpha_1\boldsymbol{Q} + \frac{\mathrm{i}\alpha_0\sigma_3}{2}(\mathrm{i}\boldsymbol{Q}^2 - \boldsymbol{Q}_x),
\end{aligned}$$

where $\alpha_i \in \mathbb{R}\,(i = 0,1,2)$.

For the t-equation

$$\begin{aligned}
&\lambda^5 : \sigma_3 \boldsymbol{D}_0^{\text{off}} = 0,\\
&\lambda^4 : -8\mathrm{i}\sigma_3 \boldsymbol{D}_1^{\text{off}} + [4\boldsymbol{Q}, \boldsymbol{D}_0] = 0,\\
&\lambda^3 : -8\mathrm{i}\sigma_3 \boldsymbol{D}_2^{\text{off}} + [4\boldsymbol{Q}, \boldsymbol{D}_1] + [2\mathrm{i}\sigma_3(\boldsymbol{Q}_x - \boldsymbol{Q}^2), \boldsymbol{D}_0] = 0,\\
&\lambda^2 : \boldsymbol{D}_{0,t} - [4\boldsymbol{Q}, \boldsymbol{D}_2] - [2\mathrm{i}\sigma_3(\boldsymbol{Q}_x - \boldsymbol{Q}^2), \boldsymbol{D}_1]\\
&\qquad - [2\boldsymbol{Q}^3 - \boldsymbol{Q}_{xx}, \boldsymbol{D}_0] = 0,\\
&\lambda^1 : \boldsymbol{D}_{1,t} - [2\mathrm{i}\sigma_3(\boldsymbol{Q}_x - \boldsymbol{Q}^2), \boldsymbol{D}_2] - [2\boldsymbol{Q}^3 - \boldsymbol{Q}_{xx}, \boldsymbol{D}_1] = 0,\\
&\lambda^0 : \boldsymbol{D}_{2,t} - [2\boldsymbol{Q}^3 - \boldsymbol{Q}_{xx}, \boldsymbol{D}_2] = 0.
\end{aligned}$$

From this, we obtain $\alpha_{0,t} = \alpha_{1,t} = 0$, and

$$\boldsymbol{Q}_t + 4\alpha_2\boldsymbol{Q}_x + 4\mathrm{i}\alpha_1\sigma_3\boldsymbol{Q}^3 - 4\alpha_1^2\boldsymbol{Q}_x + 8\mathrm{i}\alpha_1\alpha_2\sigma_3\boldsymbol{Q} = 0. \tag{10}$$

Combining the above assumptions, the determinant of the matrix $\boldsymbol{D}(x,t;\lambda)$ can be written as

$$\begin{aligned}
&\det(\boldsymbol{D}(x,t;\lambda)) = q(x,t;\lambda)^2 - w(x,t;\lambda)m(x,t;\lambda) = P(\lambda),\\
&P(\lambda) := \prod_{i=1}^{4}(\lambda - \lambda_i) = \lambda^4 - s_1\lambda^3 + s_2\lambda^2 - s_3\lambda + s_4,
\end{aligned} \tag{11}$$

where λ_i are the roots of the polynomial, and the root coefficients s_i are related to the phase velocity of the background wave. Through the symmetry relation and the existence and uniqueness of solutions to ordinary differential equations, we know that the solution satisfies $\boldsymbol{D}(x,t;\lambda) = -\boldsymbol{D}^{\dagger}(x,t;\lambda)$. Furthermore, we can obtain $\alpha_0 = 1$. Let $\mu(x,t) := -\mathrm{i}(\ln\psi)_x/2 - \alpha_1$, $\nu = |\psi|^2$. Then $q(x,t;\lambda)$, $w(x,t;\lambda)$, and $m(x,t;\lambda)$ can be represented by the following polynomials and are consistent with the results of Eq. (8)

$$\begin{aligned}
&q(x,t;\lambda) = \lambda^2 + q_1(x,t)\lambda + q_2(x,t) = \lambda^2 + \alpha_1\lambda + \alpha_2,\\
&w(x,t;\lambda) = -m^*(x,t;\lambda^*) = \psi(\lambda - \mu).
\end{aligned} \tag{12}$$

By comparing the coefficients of λ on both sides of Eq. (11), we obtain

$$\begin{aligned}
&s_1 = -2\alpha_1, \quad s_2 = \alpha_1^2 + 2\alpha_2 + \nu,\\
&s_3 = -2\alpha_1\alpha_2 + \nu(\mu + \mu^*), \quad s_4 = \alpha_2^2 + \nu\mu\mu^*,
\end{aligned} \tag{13}$$

and two quantitative relationships concerning μ, μ^*, and ν

$$\mu + \mu^* = \frac{s_1}{2} - \frac{g}{\nu}, \quad \mu\mu^* = \frac{1}{4\nu}(4s_4 - \nu^2 + 2h\nu - h^2). \tag{14}$$

The other variables involved are $g = \frac{s_1^2}{4} - s_2 + 2\nu$ and $h = \frac{s_1^3}{4} - s_1 s_2 + s_3$. According to the above equations, the expressions for $\psi^*\alpha_1$ and $\psi\alpha_2^*$ can be obtained as

$$\mu, \mu^* = \frac{s_1}{4} - \frac{g \pm \mathrm{i}\sqrt{-R(\nu)}}{2\nu}, \tag{15}$$

where

$$R(\nu) = \nu^3 + \left(\frac{s_1^2}{4} - 2h\right)\nu^2 + (h^2 - s_1 g - 4s_4)\nu + g^2. \tag{16}$$

If there exists a root ν_1 such that $R(\nu_1) = 0$, then $\det(D(x,t;\lambda))$ can be factorized as

$$\begin{aligned}
&\left[\lambda^2 + (\mathrm{i}\alpha_1 - \mathrm{i}\sqrt{\nu_1})\lambda + \left(\mathrm{i}\alpha_2 - \frac{\mathrm{i}\nu_1}{2}\right) - \mathrm{i}\sqrt{\nu_1}\mu\right]\\
&\times\left[\lambda^2 + (\mathrm{i}\alpha_1 + \mathrm{i}\sqrt{\nu_1})\lambda + \left(\mathrm{i}\alpha_2 - \frac{\mathrm{i}\nu_1}{2}\right) - \mathrm{i}\sqrt{\nu_1}\mu\right].
\end{aligned}$$

Therefore, $\mathrm{i}\alpha_1 - \mathrm{i}\sqrt{\nu_1} = -\lambda_1 - \lambda_3$, $\mathrm{i}\alpha_1 + \mathrm{i}\sqrt{\nu_1} = -\lambda_2 - \lambda_4$ and $\nu_1 = -\frac{1}{4}(\lambda_1 + \lambda_3 - \lambda_2 - \lambda_4)^2$. Similarly, for the other two roots ν_2 and ν_3, we can obtain

$$\begin{aligned}
\nu_2 &= -\frac{1}{4}(\lambda_1 + \lambda_4 - \lambda_2 - \lambda_3)^2,\\
\nu_3 &= -\frac{1}{4}(\lambda_1 + \lambda_2 - \lambda_3 - \lambda_4)^2.
\end{aligned}$$

We utilize the effective integration technique.[56] Under the periodic wave background, q_1 is related to the phase velocity of the periodic wave. In this paper, for the sake of simplicity, we set $q_1 = 0$. The case for $q_1 \neq 0$ can be given in the same way as the case for $q_1 = 0$. To satisfy $q_1 = 0$ and $\nu \geq 0$, the four zeros λ_i must consist of two pairs of complex conjugates $\lambda_{1,3} = b \pm \mathrm{i}c$ and $\lambda_{2,4} = -b \pm \mathrm{i}d$, where b, c, and d are positive real numbers, and the coefficients ν_i and s_i $(i = 1,2,3,4)$ can be simplified as

$$\begin{aligned}
&\nu_1 = -4b^2, \quad \nu_2 = (c-d)^2, \quad \nu_3 = (c+d)^2,\\
&s_1 = 0, \quad s_2 = \frac{\nu_1 + \nu_2 + \nu_3}{2}, \quad s_3 = \sqrt{-\nu_1\nu_2\nu_3},\\
&s_4 = \frac{\nu_1^2 - 2(\nu_2 + \nu_3)\nu_1 + (\nu_2 - \nu_3)^2}{16}.
\end{aligned} \tag{17}$$

Below, we will see that the parameters ν_1, ν_2, and ν_3 determine the dynamic characteristics of the solution ψ. Due to

the aforementioned relationship between v_i $(i=1,2,3)$ and λ_i $(i=1,2,3,4)$, the parameters λ_i also determine the dynamic characteristics of the solution ψ. We proceed to derive the Dubrovin-type equations corresponding to $\mu(x,t)$. Applying Eqs. (8) and (9) and setting $\lambda=\mu$, we deduce the expressions for the partial derivatives of μ with respect to x and t

$$\begin{aligned}\mu_x &= -2\mathrm{i}f(\mu) = -2\mathrm{i}\sqrt{P(\mu)},\\ \mu_t &= -2\mathrm{i}(2h-s_1^2)\sqrt{P(\mu)}.\end{aligned} \tag{18}$$

Furthermore, from Eqs. (10) and (15), along with the relationship $\mu-\mu^*=-\frac{\mathrm{i}}{2}\frac{v_x}{v}$, we can obtain

$$v_t=(s_1^2-2h)v_x=2\mathrm{i}(s_1^2-2h)\sqrt{R(v)}. \tag{19}$$

It can be obtained that the three roots satisfy the quantitative relationship $v_1\le 0\le v_2\le v_3$. Through simple mathematical analysis of the differential equation (19), we find that v is a periodic function on the interval $[v_2,v_3]$, which can be represented by Jacobi elliptic functions as

$$v(x-2s_2t)=v_3+(v_2-v_3)\,\mathrm{sn}^2\left(\sqrt{v_3-v_1}(x-2s_2t)\mid k^2\right), \tag{20}$$

where $k=\sqrt{(v_3-v_2)/(v_3-v_1)}$. According to the above equation, the traveling wave transformation $\xi=x-2s_2t$ can be adopted. From Eqs. (10), (15), and (19), we obtain

$$\psi_x=2\mathrm{i}\mu\psi,\quad \psi_t=-(4v-2h)\psi_x+2v_x\psi. \tag{21}$$

According to Eqs. (19)–(21), we can deduce the expression for the function $\psi(\xi,t)$ as

$$\begin{aligned}\psi(\xi,t) &= \sqrt{v(\xi)}\exp\left(-\mathrm{i}s_3\int_0^{\xi}\frac{\mathrm{d}s}{v(s)}-4\mathrm{i}s_3t\right)\\ &= \sqrt{v_3+(v_2-v_3)\,\mathrm{sn}^2\left(\sqrt{v_3-v_1}\xi\mid m\right)}\\ &\quad\times\exp\left(-\mathrm{i}s_3\int_0^{\xi}\frac{\mathrm{d}s}{v(s)}-4\mathrm{i}s_3t\right).\end{aligned} \tag{22}$$

2.2. Fundamental solutions of the Lax pair and their Theta function representations

To find the corresponding solutions of the Lax pair, we introduce the notation $y^2(\xi,t;\lambda)=-\det(\boldsymbol{D}(\xi,t;\lambda))$, where $y^2(\xi,t;\lambda)=q(\xi,t;\lambda)+w(\xi,t;\lambda)m(\xi,t;\lambda)$. Therefore, $\boldsymbol{K}_1(\xi,t;\lambda)=(1,r_1(\xi,t;\lambda))^{\mathrm{T}}$ and $\boldsymbol{K}_2(\xi,t;\lambda)=(1,r_2(\xi,t;\lambda))^{\mathrm{T}}$ are the kernels of the matrices $\boldsymbol{D}(\xi,t;\lambda)-\mathrm{i}y\mathbb{I}$ and $\boldsymbol{D}(\xi,t;\lambda)+\mathrm{i}y\mathbb{I}$, respectively, where

$$\begin{aligned}r_1(\xi,t;\lambda) &= \mathrm{i}\frac{q(\xi,t;\lambda)+y}{w(\xi,t;\lambda)}=\mathrm{i}\frac{m(\xi,t;\lambda)}{q(\xi,t;\lambda)-y},\\ r_2(\xi,t;\lambda) &= \mathrm{i}\frac{\mathrm{i}q(\xi,t;\lambda)-y}{w(\xi,t;\lambda)}=\mathrm{i}\frac{m(\xi,t;\lambda)}{q(\xi,t;\lambda)+y}.\end{aligned} \tag{23}$$

Assuming that the Lax pair (2) has the initial condition $\Phi(0,0;\lambda)=\mathbb{I}$ and that there exists a fundamental matrix solution $\hat{\Phi}(x,t;\lambda)$, the matrices $\hat{\Phi}(\xi,t;\lambda)\boldsymbol{D}(0,0;\lambda)$ and $\boldsymbol{D}(\xi,t;\lambda)\hat{\Phi}(\xi,t;\lambda)$ are also matrix solutions of the Lax pair (2). By the existence and uniqueness of solutions to ordinary differential equations, we obtain $\hat{\Phi}(\xi,t;\lambda)\boldsymbol{D}(0,0;\lambda)=\boldsymbol{D}(\xi,t;\lambda)\hat{\Phi}(\xi,t;\lambda)$. Furthermore, let us reconsider the solution $\Phi(x,t;\lambda)=(\Psi_1(\xi,t;\lambda),\Psi_2(\xi,t;\lambda))$. Since the Lax pair is linear, we can normalize the first components of the vector solutions $\Psi_1(0,0;\lambda)$ and $\Psi_2(0,0;\lambda)$ to unity and set their second components to $\varphi_1(0,0;\lambda)$ and $\varphi_2(0,0;\lambda)$, respectively. In other words

$$\Phi(x,t;\lambda)=\hat{\Phi}(x,t;\lambda)(\boldsymbol{K}_1(0,0;\lambda),\boldsymbol{K}_2(0,0;\lambda)).$$

Based on this, we obtain $[\boldsymbol{D}(x,t;\lambda)-\mathrm{i}y\mathbb{I}]\Phi(x,t;\lambda)=0$, and hence

$$r_i(x,t;\lambda)=\frac{\varphi_i(x,t;\lambda)}{\phi_i(x,t;\lambda)},\quad i=1,2.$$

Since $q(x,t;\lambda)$ and $w(x,t;\lambda)$ are known, the functions $\varphi_i(x,t;\lambda)$ for $i=1,2$ can be obtained. The remaining unknown variables of the Lax pair are $\phi_i(x,t;\lambda)$ for $i=1,2$. In fact, based on the previously known variables, $\phi_i(x,t;\lambda)$ can be obtained by integration

$$\begin{aligned}\phi_{1,\xi} &= (-\mathrm{i}\lambda+\psi r_1)\phi_1,\\ \phi_{1,t} &= \left[-4\mathrm{i}\lambda^3+2\mathrm{i}\lambda v+(4\lambda^2\psi+2\mathrm{i}\lambda\psi_\xi-2\psi v-\psi_{\xi\xi})r_1\right]\phi_1,\\ \phi_{2,\xi} &= (-\mathrm{i}\lambda+\psi r_2)\phi_2,\\ \phi_{2,t} &= \left[-4\mathrm{i}\lambda^3+2\mathrm{i}\lambda v+(4\lambda^2\psi+2\mathrm{i}\lambda\psi_\xi\right.\\ &\quad\left.-2\psi v-\psi_{\xi\xi})r_2\right]\phi_2.\end{aligned} \tag{24}$$

Substituting Eq. (12) into Eq. (24) yields

$$\begin{aligned}\phi_1(\xi,t;\lambda) &= \sqrt{\frac{v(\xi)-\beta_1}{v(0)-\beta_1}}\exp(\theta_1),\\ \theta_1 &= \mathrm{i}\int_0^{\xi}\frac{C_1\,\mathrm{d}s}{v(s)-\beta_1}+\mathrm{i}\lambda\xi+\mathrm{i}(4y\lambda-2s_3)t,\\ \phi_2(\xi,t;\lambda) &= \sqrt{\frac{v(\xi)-\beta_2}{v(0)-\beta_2}}\exp(\theta_2),\\ \theta_2 &= \mathrm{i}\int_0^{\xi}\frac{C_2\,\mathrm{d}s}{v(s)-\beta_2}+\mathrm{i}\lambda\xi-\mathrm{i}(4y\lambda+2s_3)t,\end{aligned} \tag{25}$$

where $C_i=2\lambda\beta_i-s_3$, $\beta_{1,2}=2(\lambda^2+\frac{s_2}{2}\mp y)$. Through steps similar to those used to obtain the first set of solutions for the Lax pair, we can also obtain another set of solutions, as shown below:

$$\begin{aligned}\varphi_1(\xi,t;\lambda) &= -\sqrt{\frac{v(0)-\beta_2}{v(0)-\beta_1}}\sqrt{\frac{v(\xi)-\beta_2}{v(0)-\beta_2}}\exp(-\theta_2),\\ \varphi_2(\xi,t;\lambda) &= -\sqrt{\frac{v(0)-\beta_1}{v(0)-\beta_2}}\sqrt{\frac{v(\xi)-\beta_1}{v(0)-\beta_1}}\exp(-\theta_1).\end{aligned} \tag{26}$$

Ignoring the constant factors in the vector solutions, we arrive at the following theorem.

Theorem 1 When ψ is given by the elliptic function (22), a fundamental solution of the Lax pair (2) can be expressed as

$$\Phi(\xi,t;\lambda)=\begin{bmatrix}\sqrt{v(\xi)-\beta_1}\,\mathrm{e}^{\theta_1} & \sqrt{v(\xi)-\beta_2}\,\mathrm{e}^{\theta_2}\\ \mathrm{i}\sqrt{v(\xi)-\beta_2}\,\mathrm{e}^{-\theta_2} & \mathrm{i}\sqrt{v(\xi)-\beta_1}\,\mathrm{e}^{-\theta_1}\end{bmatrix}, \tag{27}$$

where θ_1 and θ_2 are given in Eq. (25).

Let $\alpha=\sqrt{v_3-v_1}$ and $k=\sqrt{(v_3-v_2)/(v_3-v_1)}$. To obtain the Theta function representation of the solution, we introduce the following parameters:

$$\begin{aligned}v_1&=-\alpha^2\,\mathrm{dn}^2(K+2\mathrm{i}l\mid k^2),\\ v_2&=-k^2\alpha^2\,\mathrm{cn}^2(K+2\mathrm{i}l\mid k^2),\\ v_3&=k^2\alpha^2\,\mathrm{sn}^2(K+2\mathrm{i}l\mid k^2).\end{aligned} \tag{28}$$

According to Eqs. (20) and (28), we obtain

$$\begin{aligned}v(\xi)&=k^2\alpha^2\left(\mathrm{sn}^2(K+2\mathrm{i}l\mid k^2)-\mathrm{sn}^2(\alpha\xi\mid k^2)\right),\\ g&=\mathrm{i}k^2\alpha^3\,\mathrm{sn}(K+2\mathrm{i}l\mid k^2)\,\mathrm{cn}(K+2\mathrm{i}l\mid k^2)\,\mathrm{dn}(K+2\mathrm{i}l\mid k^2).\end{aligned}$$

Based on the addition formulas for Theta functions, we obtain

$$v(x)=\alpha^2\frac{\vartheta_2^2}{\vartheta_3^2}\frac{\vartheta_4^2\vartheta_1\left(\frac{K+2\mathrm{i}l+\alpha\xi}{2K}\right)\vartheta_1\left(\frac{K+2\mathrm{i}l-\alpha\xi}{2K}\right)}{\vartheta_4^2\left(\frac{K+2\mathrm{i}l}{2K}\right)\vartheta_4^2\left(\frac{\alpha\xi}{2K}\right)}. \tag{29}$$

Then, we obtain the Theta function representation of ψ

$$\psi=\alpha\frac{\vartheta_2\vartheta_4}{\vartheta_3}\frac{\vartheta_2\left(\frac{\alpha\xi+2\mathrm{i}l}{2K}\right)}{\vartheta_3\left(\frac{2\mathrm{i}l}{2K}\right)\vartheta_4\left(\frac{\alpha\xi}{2K}\right)}\mathrm{e}^{-\alpha Z(K+2\mathrm{i}l)\xi+4\mathrm{i}s_3t}. \tag{30}$$

Furthermore, to derive the Theta function representation of the Lax pair solutions, we need to parameterize the spectral curve $y^2=\prod_{i=1}^4(\lambda-\lambda_i)$ with the help of Eq. (18), yielding

$$\lambda(z)=\mu(\mathrm{i}(z-l)/\alpha),\quad y(z)=\frac{\alpha}{2}\frac{\mathrm{d}\mu(\mathrm{i}(z-l)/\alpha)}{\mathrm{d}z}. \tag{31}$$

We use the addition formulas for Jacobi elliptic functions to simplify $\mu(\mathrm{i}(z-l)/\alpha)$ and obtain a more convenient representation

$$\begin{aligned}\lambda(z)&=\frac{\alpha\mathrm{i}}{2}\left[\frac{-\mathrm{sn}(K+2\mathrm{i}l)\,\mathrm{cn}(K+2\mathrm{i}l)\,\mathrm{dn}(K+2\mathrm{i}l)}{\mathrm{sn}^2(K+2\mathrm{i}l)-\mathrm{sn}^2(\mathrm{i}(z-l))}\right.\\ &\quad\left.+\frac{\mathrm{sn}(\mathrm{i}(z-l))\,\mathrm{cn}(\mathrm{i}(z-l))\,\mathrm{dn}(\mathrm{i}(z-l))}{\mathrm{sn}^2(K+2\mathrm{i}l)-\mathrm{sn}^2(\mathrm{i}(z-l))}\right]\\ &=\frac{\alpha\mathrm{i}}{2}\left[\frac{\mathrm{i}\,\mathrm{dn}(\mathrm{i}(z-l))\,\mathrm{dn}(\mathrm{i}K'+K-\mathrm{i}(z+l))}{\mathrm{dn}(K+2\mathrm{i}l)}\right.\\ &\quad\left.+\frac{m\,\mathrm{sn}(K+2\mathrm{i}l)\,\mathrm{cn}(K+2\mathrm{i}l)}{\mathrm{dn}(K+2\mathrm{i}l)}\right].\end{aligned} \tag{32}$$

The above formula can be simplified to

$$\lambda(z)=\begin{cases}\dfrac{\alpha\mathrm{i}k^2}{2}\dfrac{\mathrm{sn}(\mathrm{i}(z-l))\,\mathrm{cn}(\mathrm{i}(z-l))}{\mathrm{dn}(\mathrm{i}(z-l))}, & l=\pm\dfrac{K'}{2},\\ \dfrac{\alpha\mathrm{i}}{2}\dfrac{\mathrm{sn}(\mathrm{i}(z-l))\,\mathrm{dn}(\mathrm{i}(z-l))}{\mathrm{cn}(\mathrm{i}(z-l))}, & l=0.\end{cases} \tag{33}$$

In addition, through the addition formulas for Jacobi elliptic functions, we obtain a simple formula for $\lambda^2(z)$

$$\begin{aligned}\lambda^2(z)&=\frac{\alpha^2}{4}\left[\mathrm{dn}^2(K+2\mathrm{i}l)+m-2+\mathrm{dn}^2(\mathrm{i}(z-l))\right.\\ &\quad\left.+\mathrm{dn}^2(\mathrm{i}K'+K-\mathrm{i}(z+l))\right],\end{aligned} \tag{34}$$

Thus, $y(z)$ can be rewritten as

$$y(z)=\frac{\alpha^2}{4}\left[\mathrm{dn}^2(K+\mathrm{i}K'-\mathrm{i}(z+l))-\mathrm{dn}^2(\mathrm{i}(z-l))\right]. \tag{35}$$

Based on $\beta_1=2(\lambda^2+\frac{s_2}{2}-y)$ and $\beta_2=2(\lambda^2+\frac{s_2}{2}+y)$, as well as the aforementioned results, we obtain

$$\begin{aligned}\beta_1&=2(\lambda^2(z)+s_2/2-y(z))\\ &=m\alpha^2[\mathrm{sn}^2(K+2\mathrm{i}l)-\mathrm{sn}^2(\mathrm{i}(z-l))],\\ \beta_2&=2(\lambda^2(z)+s_2/2+y(z))\\ &=m\alpha^2[\mathrm{sn}^2(K+2\mathrm{i}l)-\mathrm{sn}^2(\mathrm{i}K'+K-\mathrm{i}(z+l))].\end{aligned} \tag{36}$$

From this, we obtain

$$\begin{aligned}v(x)-\beta_1&=m\alpha^2(\mathrm{sn}^2(\mathrm{i}(z-l))-\mathrm{sn}^2(\alpha\xi)),\\ v(x)-\beta_2&=m\alpha^2(\mathrm{sn}^2(\mathrm{i}K'+K-\mathrm{i}(z+l))-\mathrm{sn}^2(\alpha\xi)).\end{aligned} \tag{37}$$

According to the above equations, through calculations similar to those leading to Eq. (30), we obtain

$$\begin{aligned}\phi_1(\xi,t;z)&=\alpha\frac{\vartheta_2\vartheta_4}{\vartheta_3}\frac{\vartheta_1\left(\frac{\mathrm{i}(z-l)-\alpha\xi}{2K}\right)}{\vartheta_4\left(\frac{\mathrm{i}(z-l)}{2K}\right)\vartheta_4\left(\frac{\alpha\xi}{2K}\right)}\\ &\quad\times\mathrm{e}^{(\alpha Z(\mathrm{i}(z-l))+\mathrm{i}\lambda)\xi+\mathrm{i}(4y\lambda-2s_3)t},\\ \phi_2(\xi,t;z)&=\alpha\frac{\vartheta_2\vartheta_4}{\vartheta_3}\frac{\vartheta_1\left(\frac{\mathrm{i}K'-K-\mathrm{i}(z+l)-\alpha\xi}{2K}\right)}{\vartheta_4\left(\frac{\mathrm{i}K'-K-\mathrm{i}(z+l)}{2K}\right)\vartheta_4\left(\frac{\alpha\xi}{2K}\right)}\\ &\quad\times\mathrm{e}^{(-\mathrm{i}\frac{\alpha\pi}{2K}-\alpha Z(\mathrm{i}K'+K-\mathrm{i}(z+l))+\mathrm{i}\lambda)x-\mathrm{i}(4y\lambda+2s_3)t}.\end{aligned} \tag{38}$$

Through the addition formulas for Theta functions (B6), we obtain

$$\begin{aligned}\lambda(z)-\mu(\xi)&=\frac{\alpha\mathrm{i}\vartheta_2\vartheta_4}{2\vartheta_3}\\ &\quad\times\frac{\vartheta_1\left(\frac{\mathrm{i}(z-l)-\alpha\xi}{2K}\right)\vartheta_3\left(\frac{2\mathrm{i}l}{2K}\right)\vartheta_3\left(\frac{\mathrm{i}(z+l)+\alpha\xi}{2K}\right)}{\vartheta_2\left(\frac{\mathrm{i}(z+l)}{2K}\right)\vartheta_4\left(\frac{\mathrm{i}(z-l)}{2K}\right)\vartheta_2\left(\frac{\alpha\xi+2\mathrm{i}l}{2K}\right)\vartheta_4\left(\frac{\alpha\xi}{2K}\right)},\\ \lambda(z)-\mu^*(\xi)&=\frac{\alpha\mathrm{i}\vartheta_2\vartheta_4}{2\vartheta_3}\\ &\quad\times\frac{\vartheta_1\left(\frac{\mathrm{i}(z-l)+\alpha\xi}{2K}\right)\vartheta_3\left(\frac{2\mathrm{i}l}{2K}\right)\vartheta_3\left(\frac{\mathrm{i}(z+l)-\alpha\xi}{2K}\right)}{\vartheta_2\left(\frac{\mathrm{i}(z+l)}{2K}\right)\vartheta_4\left(\frac{\mathrm{i}(z-l)}{2K}\right)\vartheta_2\left(\frac{\alpha\xi-2\mathrm{i}l}{2K}\right)\vartheta_4\left(\frac{\alpha\xi}{2K}\right)}.\end{aligned} \tag{39}$$

According to Eqs. (37), (39), and $r_i=\frac{\varphi_i}{\phi_i}$, it follows that

$$r_1(\xi,t;z)=-\frac{\vartheta_4\left(\frac{\mathrm{i}(z-l)}{2K}\right)\vartheta_3\left(\frac{\mathrm{i}(z+l)-\alpha\xi}{2K}\right)}{\vartheta_2\left(\frac{\mathrm{i}(z+l)}{2K}\right)\vartheta_1\left(\frac{\mathrm{i}(z-l)-\alpha\xi}{2K}\right)}\mathrm{e}^{\alpha Z(2\mathrm{i}l+K)\xi-4\mathrm{i}s_3t},$$

$$r_2(\xi,t;z) = -\frac{\vartheta_2\left(\frac{\mathrm{i}(z+l)}{2K}\right)\vartheta_1\left(\frac{\mathrm{i}(z-l)+\alpha\xi}{2K}\right)}{\vartheta_4\left(\frac{\mathrm{i}(z-l)}{2K}\right)\vartheta_3\left(\frac{\mathrm{i}(z+l)+\alpha\xi}{2K}\right)} \times \mathrm{e}^{\alpha\left(Z(2\mathrm{i}l+K)+\frac{\mathrm{i}\pi}{2K}\right)\xi-4\mathrm{i}s_3t}, \tag{40}$$

thus

$$\begin{aligned}\psi_1(\xi,t;z) &= -\alpha\frac{\vartheta_2\vartheta_4}{\vartheta_3}\frac{\vartheta_3\left(\frac{\mathrm{i}(z+l)-\alpha\xi}{2K}\right)}{\vartheta_2\left(\frac{\mathrm{i}(z+l)}{2K}\right)\vartheta_4\left(\frac{\alpha\xi}{2K}\right)} \times E_1(\xi,t;z)E_3(\xi,t;z),\\ \psi_2(\xi,t;z) &= -\alpha\frac{\vartheta_2\vartheta_4}{\vartheta_3}\frac{\vartheta_1\left(\frac{\mathrm{i}(z-l)+\alpha\xi}{2K}\right)}{\vartheta_4\left(\frac{\mathrm{i}(z-l)}{2K}\right)\vartheta_4\left(\frac{\alpha\xi}{2K}\right)} \times E_2(\xi,t;z)E_3(\xi,t;z),\end{aligned} \tag{41}$$

where

$$\begin{aligned}E_1(\xi,t;z) &= \exp\left[(\alpha Z(\mathrm{i}(z-l))+\mathrm{i}\lambda)\xi+\mathrm{i}(4y\lambda-2s_3)t\right],\\ E_2(\xi,t;z) &= \exp\left[\left(-\mathrm{i}\frac{\alpha\pi}{2K}-\alpha Z(\mathrm{i}(z+l)+K+\mathrm{i}K')+\mathrm{i}\lambda\right)\xi\right.\\ &\quad \left.-\mathrm{i}(4y\lambda+2s_3)t\right],\\ E_3(\xi,t;z) &= \exp\left[\alpha\left(Z(2\mathrm{i}l+K)+\frac{\mathrm{i}\pi}{2K}\right)\xi-4\mathrm{i}s_3t\right].\end{aligned} \tag{42}$$

Based on Eqs. (38), (40), and (41), we can draw the following conclusion.

Theorem 2 When ψ is given by Eq. (30), the vector solution of the Lax pair for Eq. (2) can be expressed in terms of Theta functions as follows:

$$\begin{bmatrix}\phi_1(\xi,t;z)\\ \varphi_1(\xi,t;z)\end{bmatrix} = \alpha\frac{\vartheta_2\vartheta_4}{\vartheta_3\vartheta_4\left(\frac{\alpha\xi}{2K}\right)}E_1(\xi,t;z) \times\begin{bmatrix}\frac{\vartheta_1\left(\frac{\mathrm{i}(z-l)-\alpha\xi}{2K}\right)}{\vartheta_4\left(\frac{\mathrm{i}(z-l)}{2K}\right)}\\ \mathrm{i}\frac{\vartheta_3\left(\frac{\mathrm{i}(z+l)-\alpha\xi}{2K}\right)}{\vartheta_2\left(\frac{\mathrm{i}(z+l)}{2K}\right)}E_3(\xi,t;z)\end{bmatrix}, \tag{43}$$

$$\begin{bmatrix}\phi_2(\xi,t;z)\\ \varphi_2(\xi,t;z)\end{bmatrix} = \alpha\frac{\vartheta_2\vartheta_4}{\vartheta_3\vartheta_4\left(\frac{\alpha\xi}{2K}\right)}E_2(\xi,t;z) \times\begin{bmatrix}\frac{\vartheta_3\left(\frac{\mathrm{i}(z+l)+\alpha\xi}{2K}\right)}{\vartheta_2\left(\frac{\mathrm{i}(z+l)}{2K}\right)}\\ \mathrm{i}\frac{\vartheta_1\left(\frac{\mathrm{i}(z-l)+\alpha\xi}{2K}\right)}{\vartheta_4\left(\frac{\mathrm{i}(z-l)}{2K}\right)}E_3(\xi,t;z)\end{bmatrix}. \tag{44}$$

3. Elliptic-localized wave solutions

In this section, we obtain elliptic-localized wave solutions by applying the n-th-order Darboux transformation, while simultaneously obtaining the Theta function representations of the solutions of the cmKdV equation.

We consider the localized wave solutions obtained through linear combinations of the two sets of Lax pair solutions Eqs. (43) and (44)

$$\begin{aligned}\Phi(\xi,t;z_j) &= \begin{bmatrix}\phi_1(\xi,t;z_j)\\ \varphi_1(\xi,t;z_j)\end{bmatrix}+\alpha_j\begin{bmatrix}\phi_2(\xi,t;z_j)\\ \varphi_2(\xi,t;z_j)\end{bmatrix}\\ &= \alpha\frac{\vartheta_2\vartheta_4}{\vartheta_3\vartheta_4\left(\frac{\alpha\xi}{2K}\right)}\left(E_1\begin{bmatrix}\frac{\vartheta_1\left(\frac{\mathrm{i}(z_j-l)-\alpha\xi}{2K}\right)}{\vartheta_4\left(\frac{\mathrm{i}(z_j-l)}{2K}\right)}\\ -\frac{\vartheta_3\left(\frac{\mathrm{i}(z_j+l)-\alpha\xi}{2K}\right)}{\vartheta_2\left(\frac{\mathrm{i}(z_j+l)}{2K}\right)}E_3\end{bmatrix}+\alpha_jE_2\begin{bmatrix}\frac{\vartheta_3\left(\frac{\mathrm{i}(z_j+l)+\alpha\xi}{2K}\right)}{\vartheta_2\left(\frac{\mathrm{i}(z_j+l)}{2K}\right)}\\ -\frac{\vartheta_1\left(\frac{\mathrm{i}(z_j-l)+\alpha\xi}{2K}\right)}{\vartheta_4\left(\frac{\mathrm{i}(z_j-l)}{2K}\right)}E_3\end{bmatrix}\right).\end{aligned} \tag{45}$$

At the same time, we present the complex conjugate of solution Eq. (45)

$$\begin{aligned}\Phi^*(\xi,t;z_i) &= \begin{bmatrix}\phi_1(\xi,t;z_i)\\ \varphi_1(\xi,t;z_i)\end{bmatrix}+\alpha_i^*\begin{bmatrix}\phi_2(\xi,t;z_i)\\ \varphi_2(\xi,t;z_i)\end{bmatrix}\\ &= \alpha\frac{\vartheta_2\vartheta_4}{\vartheta_3\vartheta_4\left(\frac{\alpha\xi}{2K}\right)}\left(E_1^*\begin{bmatrix}\frac{\vartheta_1\left(\frac{\mathrm{i}(z_i^*-l)-\alpha\xi}{2K}\right)}{\vartheta_4\left(\frac{\mathrm{i}(z_i^*-l)}{2K}\right)}\\ -\frac{\vartheta_3\left(\frac{\mathrm{i}(z_i^*+l)-\alpha\xi}{2K}\right)}{\vartheta_2\left(\frac{\mathrm{i}(z_i^*+l)}{2K}\right)}E_3\end{bmatrix}+\alpha_i^*E_2^*\begin{bmatrix}\frac{\vartheta_3\left(\frac{\mathrm{i}(z_i^*+l)+\alpha\xi}{2K}\right)}{\vartheta_2\left(\frac{\mathrm{i}(z_i^*+l)}{2K}\right)}\\ -\frac{\vartheta_1\left(\frac{\mathrm{i}(z_i^*-l)+\alpha\xi}{2K}\right)}{\vartheta_4\left(\frac{\mathrm{i}(z_i^*-l)}{2K}\right)}E_3\end{bmatrix}\right),\end{aligned} \tag{46}$$

where α_j and α_i are complex constants, and E_1, E_2, and E_3 are defined in Eq. (42).

Through the Darboux transformation (A4), the general solution can be obtained. The solution obtained by the n-th-order Darboux transformation can be expressed as

$$\psi_n(\xi,t)=\psi(\xi)-[\boldsymbol{\Phi}_1,\boldsymbol{\Phi}_2,\ldots,\boldsymbol{\Phi}_n]\boldsymbol{U}^{-1}\begin{bmatrix}\boldsymbol{\Phi}_1^*\\ \boldsymbol{\Phi}_2^*\\ \vdots\\ \boldsymbol{\Phi}_n^*\end{bmatrix}, \tag{47}$$

where $\psi(\xi)$ is given in Eq. (30) and

$$\boldsymbol{U}=\left(\frac{\boldsymbol{\Phi}^{\dagger}(z_i)\boldsymbol{\Phi}(z_j)}{2(\lambda(z_j)-\lambda(z_i^*))}\right)_{1\le i,j\le n}. \tag{48}$$

Next, we utilize Eqs. (45) and (46) to express the components in Eq. (48)

$$\boldsymbol{\Phi}^{\dagger}(z_i)\boldsymbol{\Phi}(z_j)=\frac{\alpha^2\vartheta_2^2\vartheta_4^2}{\vartheta_3^2\vartheta_4^2\left(\frac{\alpha\xi}{2K}\right)}\left(-E_1(z_j)E_1^*(z_i)\Delta_1+\alpha_i^*E_1(z_j)E_2^*(z_i)\Delta_2-\alpha_jE_2(z_j)E_1^*(z_i)\Delta_3+\alpha_i^*\alpha_jE_2(z_j)E_2^*(z_i)\Delta_4\right), \tag{49}$$

where

$$\Delta_1=-\frac{\vartheta_3\left(\frac{2\mathrm{i}l}{2K}\right)\vartheta_3\left(\frac{\mathrm{i}(z_i^*+z_j)}{2K}\right)\vartheta_4\left(\frac{\alpha_1\xi-\mathrm{i}(z_j-z_i^*)}{2K}\right)\vartheta_4\left(\frac{\alpha_1\xi}{2K}\right)}{\vartheta_4\left(\frac{\mathrm{i}(z_i^*-l)}{2K}\right)\vartheta_4\left(\frac{\mathrm{i}(z_j-l)}{2K}\right)\vartheta_2\left(\frac{\mathrm{i}(z_i^*+l)}{2K}\right)\vartheta_2\left(\frac{\mathrm{i}(z_j+l)}{2K}\right)},\quad \Delta_2=-\mathrm{e}^{\frac{\mathrm{i}\alpha\pi\xi}{2K}}\frac{\vartheta_3\left(\frac{2\mathrm{i}l}{2K}\right)\vartheta_1\left(\frac{\mathrm{i}(z_j-z_i^*)}{2K}\right)\vartheta_4\left(\frac{\alpha x}{2K}\right)\vartheta_2\left(\frac{\alpha x-\mathrm{i}(z_i^*+z_j)}{2K}\right)}{\vartheta_4\left(\frac{\mathrm{i}(z_i^*-l)}{2K}\right)\vartheta_4\left(\frac{\mathrm{i}(z_j-l)}{2K}\right)\vartheta_4\left(\frac{\mathrm{i}(z_j+l)}{2K}\right)\vartheta_4\left(\frac{\mathrm{i}(z_i^*+l)}{2K}\right)},$$

$$\Delta_3=\mathrm{e}^{\frac{\mathrm{i}\alpha\pi\xi}{2K}}\frac{\vartheta_3\left(\frac{2\mathrm{i}l}{2K}\right)\vartheta_1\left(\frac{\mathrm{i}(z_i^*-z_j)}{2K}\right)\vartheta_4\left(\frac{\alpha x}{2K}\right)\vartheta_2\left(\frac{\alpha x+\mathrm{i}(z_i^*+z_j)}{2K}\right)}{\vartheta_4\left(\frac{\mathrm{i}(z_i^*-l)}{2K}\right)\vartheta_4\left(\frac{\mathrm{i}(z_j-l)}{2K}\right)\vartheta_2\left(\frac{\mathrm{i}(z_j+l)}{2K}\right)\vartheta_2\left(\frac{\mathrm{i}(z_i^*+l)}{2K}\right)},\quad \Delta_4=\frac{\vartheta_3\left(\frac{2\mathrm{i}l}{2K}\right)\vartheta_3\left(\frac{\mathrm{i}(z_j+z_i^*)}{2K}\right)\vartheta_4\left(\frac{\alpha x}{2K}\right)\vartheta_4\left(\frac{\alpha x-\mathrm{i}(z_i^*-z_j)}{2K}\right)}{\vartheta_4\left(\frac{\mathrm{i}(z_i^*-l)}{2K}\right)\vartheta_4\left(\frac{\mathrm{i}(z_j-l)}{2K}\right)\vartheta_2\left(\frac{\mathrm{i}(z_j+l)}{2K}\right)\vartheta_2\left(\frac{\mathrm{i}(z_i^*+l)}{2K}\right)}.$$

Through the addition formulas for Theta functions, we obtain

$$2(\lambda(z_j)-\lambda(z_i^*))=\alpha\mathrm{i}\frac{\vartheta_2\vartheta_4}{\vartheta_3}\frac{\vartheta_3\left(\frac{2\mathrm{i}l}{2K}\right)\vartheta_1\left(\frac{\mathrm{i}(z_j-z_i^*)}{2K}\right)\vartheta_3\left(\frac{\mathrm{i}(z_j+z_i^*)}{2K}\right)}{\vartheta_2\left(\frac{\mathrm{i}(z_j+l)}{2K}\right)\vartheta_4\left(\frac{\mathrm{i}(z_j-l)}{2K}\right)\vartheta_2\left(\frac{\mathrm{i}(z_i^*+l)}{2K}\right)\vartheta_4\left(\frac{\mathrm{i}(z_i^*-l)}{2K}\right)}. \tag{50}$$

From this, we obtain

$$\frac{\boldsymbol{\Phi}^{\dagger}(z_i)\boldsymbol{\Phi}(z_j)}{2(\lambda(z_j)-\lambda(z_i^*))}=\frac{1}{\alpha\mathrm{i}}\frac{\vartheta_3\vartheta_4\left(\frac{\alpha\xi}{2K}\right)}{\vartheta_2\vartheta_4}O_{i,j}, \tag{51}$$

where

$$\begin{aligned}O_{i,j}=\;&E_1(z_j)E_1^*(z_i)\frac{\vartheta_4\left(\frac{\alpha\xi+\mathrm{i}(z_i^*-z_j)}{2K}\right)}{\vartheta_1\left(\frac{\mathrm{i}(z_j-z_i^*)}{2K}\right)}+\alpha_i^*E_1(z_j)E_2^*(z_i)\frac{\vartheta_2\left(\frac{\alpha\xi-\mathrm{i}(z_i^*+z_j)}{2K}\right)}{\vartheta_3\left(\frac{\mathrm{i}(z_j+z_i^*)}{2K}\right)}\\&+\alpha_jE_2(z_j)E_1^*(z_i)\frac{\vartheta_2\left(\frac{\alpha\xi+\mathrm{i}(z_i^*+z_j)}{2K}\right)}{\vartheta_3\left(\frac{\mathrm{i}(z_j+z_i^*)}{2K}\right)}+\alpha_i^*\alpha_jE_2(z_j)E_2^*(z_i)\frac{\vartheta_4\left(\frac{\alpha\xi-\mathrm{i}(z_i^*-z_j)}{2K}\right)}{\vartheta_1\left(\frac{\mathrm{i}(z_j-z_i^*)}{2K}\right)}.\end{aligned} \tag{52}$$

With the help of the above equations and the addition formulas for Theta functions, we obtain the expression for $H_{i,j}$

$$\begin{aligned}H_{i,j}=\;&E_1(z_j)E_1^*(z_i)\frac{\vartheta_2\left(\frac{\mathrm{i}(z_j+l)}{2K}\right)\vartheta_4\left(\frac{\mathrm{i}(z_i^*-l)}{2K}\right)}{\vartheta_4\left(\frac{\mathrm{i}(z_j-l)}{2K}\right)\vartheta_2\left(\frac{\mathrm{i}(z_i^*+l)}{2K}\right)}\frac{\vartheta_2\left(\frac{\mathrm{i}(z_i^*-z_j)+2\mathrm{i}l+\alpha\xi}{2K}\right)}{\vartheta_1\left(\frac{\mathrm{i}(z_i^*-z_j)}{2K}\right)}\\&+\alpha_i^*E_1(z_j)E_2^*(z_i)\frac{\vartheta_2\left(\frac{\mathrm{i}(z_j+l)}{2K}\right)\vartheta_2\left(\frac{\mathrm{i}(z_i^*+l)}{2K}\right)}{\vartheta_4\left(\frac{\mathrm{i}(z_j-l)}{2K}\right)\vartheta_4\left(\frac{\mathrm{i}(z_i^*-l)}{2K}\right)}\frac{\vartheta_4\left(\frac{-\mathrm{i}(z_i^*+z_j)+2\mathrm{i}l+\alpha\xi}{2K}\right)}{\vartheta_3\left(\frac{\mathrm{i}(z_i^*+z_j)}{2K}\right)}\end{aligned}$$

$$-\alpha_j E_2(z_j)E_1^*(z_i)\frac{\vartheta_4\left(\frac{\mathrm{i}(z_j-l)}{2K}\right)\vartheta_4\left(\frac{\mathrm{i}(z_i^*-l)}{2K}\right)}{\vartheta_2\left(\frac{\mathrm{i}(z_j+l)}{2K}\right)\vartheta_2\left(\frac{\mathrm{i}(z_i^*+l)}{2K}\right)}\frac{\vartheta_4\left(\frac{\mathrm{i}(z_i^*+z_j)+2\mathrm{i}l+\alpha\xi}{2K}\right)}{\vartheta_3\left(\frac{\mathrm{i}(z_i^*+z_j)}{2K}\right)}$$
$$+\alpha_j\alpha_i^* E_2(z_j)E_2^*(z_i)\frac{\vartheta_4\left(\frac{\mathrm{i}(z_j-l)}{2K}\right)\vartheta_2\left(\frac{\mathrm{i}(z_i^*+l)}{2K}\right)}{\vartheta_2\left(\frac{\mathrm{i}(z_j+l)}{2K}\right)\vartheta_4\left(\frac{\mathrm{i}(z_i^*-l)}{2K}\right)}\frac{\vartheta_2\left(\frac{\mathrm{i}(z_j-z_i^*)+2\mathrm{i}l+\alpha\xi}{2K}\right)}{\vartheta_1\left(\frac{\mathrm{i}(z_j-z_i^*)}{2K}\right)}. \tag{53}$$

Finally, by substituting Eqs. (52) and (53) into Eq. (48), we can deduce the following theorem.

Theorem 3 The localized wave solution of the cmKdV equation on a Jacobi elliptic function background is given by

$$\psi_n = \alpha\frac{\vartheta_2\vartheta_4}{\vartheta_3\vartheta_3\left(\frac{2\mathrm{i}l}{2K}\right)}\left(\frac{\vartheta_4\left(\frac{\alpha\xi}{2K}\right)}{\vartheta_2\left(\frac{\alpha\xi+2\mathrm{i}l}{2K}\right)}\right)^{n-1}\times\frac{\det(\boldsymbol{H})}{\det(\boldsymbol{O})}\mathrm{e}^{-\alpha Z(2\mathrm{i}l+K)\xi+4\mathrm{i}s_3t}, \tag{54}$$

where $\boldsymbol{O}=(O_{i,j})_{1\le i,j\le n}$ and $\boldsymbol{H}=(H_{i,j})_{1\le i,j\le n}$.

Through the above analysis, we obtain elliptic-localized wave solutions with different dynamic behaviors. Based on Theorem 3, n in the elliptic-localized wave solution ψ_n represents the total number of localized waves. Below, we present different elliptic-localized wave solutions, including elliptic soliton solutions, elliptic breather solutions, elliptic multi-soliton solutions, elliptic multi-breather solutions, and elliptic multi-soliton-multi-breather solutions, primarily taking $n=1,2$ as examples. During the solution process of the cmKdV equation, different types of localized solutions on the elliptic background can be systematically constructed by varying the matrix dimension n and the spectral parameter configuration. Here, we illustrate this with $n=1,2$.

3.1. Dynamics of elliptic-localized wave solutions on cn-type backgrounds

Taking the parameters $l=0$, $\alpha=1$, and $k=1/2$ in Eq. (54), we obtain $v_1=-0.75$, $v_2=0$, $v_3=0.25$, and $s_2=-0.25$. Furthermore, by selecting different parameters z_i and α_i, $i=1,2$, the elliptic-soliton solutions, elliptic-breather solutions, elliptic-two-soliton solutions, elliptic-soliton-breather solutions, and elliptic-two-breather solutions of the cmKdV equation on the cn-type background are presented in Figs. 1–4.

In this subsection, setting the parameters $l=0$ and $n=1$ in Eq. (54) and utilizing the transformation formulas of Theta functions, we derive a more compact expression for the elliptic-single-localized wave solution

$$\psi_1=\alpha\frac{\vartheta_2\vartheta_4}{\vartheta_3\vartheta_3\left(\frac{2\mathrm{i}l}{2K}\right)}\frac{H_1}{O_1}\mathrm{e}^{-\alpha Z(2\mathrm{i}l+K)\xi+4\mathrm{i}s_3t}, \tag{55}$$

where

$$O_1 = E_1(z_1)E_1^*(z_1)\frac{\vartheta_4\left(\frac{\alpha\xi+\mathrm{i}(z_1^*-z_1)}{2K}\right)}{\vartheta_1\left(\frac{\mathrm{i}(z_1-z_1^*)}{2K}\right)}+\alpha_1^*E_1(z_1)E_1^*(z_1)\frac{\vartheta_2\left(\frac{\alpha\xi-\mathrm{i}(z_1^*+z_1)}{2K}\right)}{\vartheta_3\left(\frac{\mathrm{i}(z_1+z_1^*)}{2K}\right)}$$
$$+\alpha_1E_2(z_1)E_1^*(z_1)\frac{\vartheta_2\left(\frac{\alpha\xi+\mathrm{i}(z_1^*+z_1)}{2K}\right)}{\vartheta_3\left(\frac{\mathrm{i}(z_1+z_1^*)}{2K}\right)}+\alpha_1^*\alpha_1E_2(z_1)E_2^*(z_1)\frac{\vartheta_4\left(\frac{\alpha\xi-\mathrm{i}(z_1^*-z_1)}{2K}\right)}{\vartheta_1\left(\frac{\mathrm{i}(z_1-z_1^*)}{2K}\right)}, \tag{56}$$

$$H_1 = E_1(z_1)E_1^*(z_1)\frac{\vartheta_2\left(\frac{\mathrm{i}(z_1+l)}{2K}\right)\vartheta_4\left(\frac{\mathrm{i}(z_1^*-l)}{2K}\right)}{\vartheta_4\left(\frac{\mathrm{i}(z_1-l)}{2K}\right)\vartheta_2\left(\frac{\mathrm{i}(z_1^*+l)}{2K}\right)}\frac{\vartheta_2\left(\frac{\mathrm{i}(z_1^*-z_1)+2\mathrm{i}l+\alpha\xi}{2K}\right)}{\vartheta_1\left(\frac{\mathrm{i}(z_1^*-z_1)}{2K}\right)}$$
$$+\alpha_1^*E_1(z_1)E_2^*(z_1)\frac{\vartheta_2\left(\frac{\mathrm{i}(z_1+l)}{2K}\right)\vartheta_2\left(\frac{\mathrm{i}(z_1^*+l)}{2K}\right)}{\vartheta_4\left(\frac{\mathrm{i}(z_1-l)}{2K}\right)\vartheta_4\left(\frac{\mathrm{i}(z_1^*-l)}{2K}\right)}\frac{\vartheta_4\left(\frac{-\mathrm{i}(z_1^*+z_1)+2\mathrm{i}l+\alpha\xi}{2K}\right)}{\vartheta_3\left(\frac{\mathrm{i}(z_1^*+z_1)}{2K}\right)}$$
$$-\alpha_1E_2(z_1)E_1^*(z_1)\frac{\vartheta_4\left(\frac{\mathrm{i}(z_1-l)}{2K}\right)\vartheta_4\left(\frac{\mathrm{i}(z_1^*-l)}{2K}\right)}{\vartheta_2\left(\frac{\mathrm{i}(z_1+l)}{2K}\right)\vartheta_2\left(\frac{\mathrm{i}(z_1^*+l)}{2K}\right)}\frac{\vartheta_4\left(\frac{\mathrm{i}(z_1^*+z_1)+2\mathrm{i}l+\alpha\xi}{2K}\right)}{\vartheta_3\left(\frac{\mathrm{i}(z_1^*+z_1)}{2K}\right)}$$
$$+\alpha_1\alpha_1^*E_2(z_1)E_2^*(z_1)\frac{\vartheta_4\left(\frac{\mathrm{i}(z_1-l)}{2K}\right)\vartheta_2\left(\frac{\mathrm{i}(z_1^*+l)}{2K}\right)}{\vartheta_2\left(\frac{\mathrm{i}(z_1+l)}{2K}\right)\vartheta_4\left(\frac{\mathrm{i}(z_1^*-l)}{2K}\right)}\frac{\vartheta_2\left(\frac{\mathrm{i}(z_1-z_1^*)+2\mathrm{i}l+\alpha\xi}{2K}\right)}{\vartheta_1\left(\frac{\mathrm{i}(z_1-z_1^*)}{2K}\right)}. \tag{57}$$

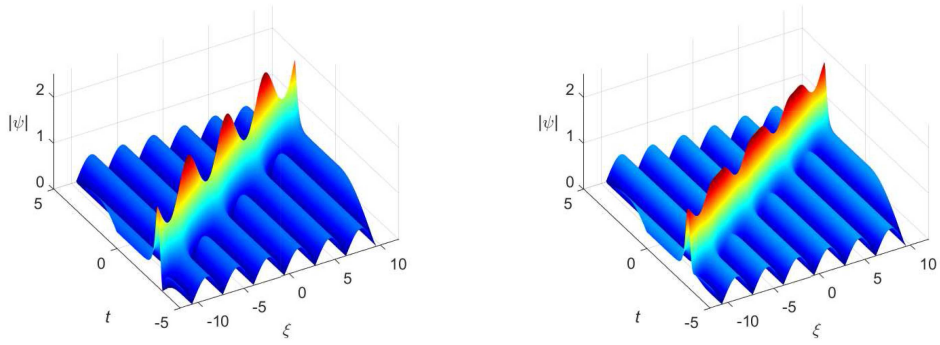


Fig. 1. Elliptic-soliton solutions of the cmKdV equation on the cn-type background. (a) $\alpha_1 = 1$ and $z_1 = K' + K\mathrm{i}/3$; (b) $\alpha_1 = \exp(\mathrm{i}\pi/3)$ and $z_1 = K' + K\mathrm{i}/3$.

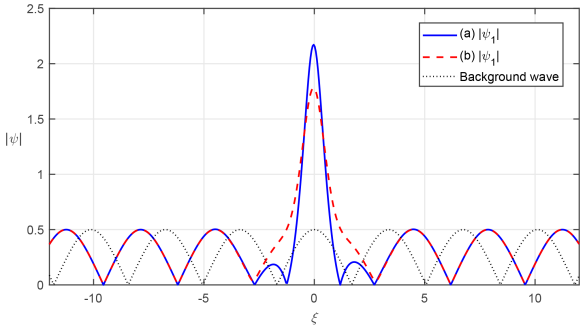


Fig. 2. Modulus cross-section profiles $|\psi_1(x,0)|$ of the elliptic-soliton solutions at $t = 0$, compared with the background wave.

When $\alpha_1 = 1$ and $z_1 = K' + K\mathrm{i}/3$, $\lambda(z_1) \approx -0.836\mathrm{i}$. Substituting these parameters into Eq. (55) yields the elliptic-soliton solution shown in Fig. 1(a), where the soliton solution reaches a maximum value of approximately 2.1716 at the origin. Since the free parameter $\alpha_1 \in \mathbb{R}$, the solution ψ_1 remains real, and the cmKdV equation reduces to the mKdV equation. When $\alpha_1 = \exp(\mathrm{i}\pi/3)$ and $z_1 = K' + K\mathrm{i}/3$, since z_1 remains unchanged, $\lambda(z_1) \approx -0.836\mathrm{i}$. Substituting these parameters into Eq. (55) yields the elliptic-soliton solution shown in Fig. 1(b), where the maximum value of the soliton solution is approximately 1.7840. Although the spectral parameter $\lambda(z_1)$ still lies on the imaginary axis, the complex-valued free parameter $\alpha_1 = \exp(\mathrm{i}\pi/3)$ makes the solution ψ_1 complex-valued, introducing phase modulation that significantly alters the amplitude profile.

Figure 2 displays a comparison between the modulus cross-section profiles $|\psi_1(x,0)|$ of the elliptic-soliton solutions under different parameters and the background wave at $t = 0$. The black dotted line represents the unperturbed background elliptic cosine wave, while the two colored curves correspond to the classical mKdV soliton and the parameter-modulated cmKdV soliton, respectively. It can be clearly observed that all soliton solutions converge to the background wave in regions far from the perturbation center, confirming the localized characteristics of these solutions on periodic backgrounds. Comparing the different curves reveals that the introduction of the complex free parameter α_1 breaks the parity symmetry of the waveform and produces a phase shift, while the complex spectral parameter further modifies the wave packet width and amplitude modulation depth of the soliton. These features indicate that the cmKdV model possesses a richer soliton dynamical structure than the traditional real-valued model.

When $\alpha_1 = 1$ and $z_1 = 3K'/4 + K\mathrm{i}/3$, the corresponding spectral parameter is $\lambda(z_1) \approx -0.504 - 0.429\mathrm{i}$, yielding the elliptic-breather solution shown in Fig. 3(a). In this case, the breather solution reaches a maximum value of approximately 1.3559 at the origin, and the wave packet exhibits periodic oscillations while propagating steadily along the x-axis. By adjusting the parameter to $z_1 = 0.5571 + 0.6743\mathrm{i}$, we obtain $\lambda(z_1) \approx -0.314 - 0.286\mathrm{i}$, which yields the elliptic-breather solution shown in Fig. 3(b). Here, the translational velocity of the breather is completely canceled, transforming it into a stationary breather with local envelope beating at a fixed position. The breather solution reaches a maximum value of approximately 1.0722 at the origin, exhibiting stronger energy concentration. By further introducing the complex parameter $\alpha_1 = 1 + 0.5\mathrm{i}$, with $z_1 = 3K'/4 + K\mathrm{i}/4$ and $\lambda(z_1) \approx -0.626 - 0.427\mathrm{i}$, we obtain the elliptic-breather solution shown in Fig. 3(c), with a maximum value of approximately 1.3338. The complex parameter α_1 introduces additional phase modulation, leading to the rotation and distortion of the phase profile of the wave packet, thereby directly altering the symmetry and amplitude profile of the breather.

Next, setting the parameters $l = 0$ and $n = 2$ in Eq. (54), we obtain the elliptic-double-localized wave solutions on the cn-type background.

When $\alpha_1 = \exp(\mathrm{i}\pi/4)$, $\alpha_2 = \exp(\mathrm{i}\pi/3)$, $z_1 = K' + 2K\mathrm{i}/9$, and $z_2 = K' + K\mathrm{i}/3$, the corresponding spectral parameters are $\lambda(z_1) \approx -1.301\mathrm{i}$ and $\lambda(z_2) \approx -0.836\mathrm{i}$. Substituting these parameters into the formula yields the elliptic-two-soliton solution shown in Fig. 4(a), with a maximum peak value of approximately 3.517. When $\alpha_1 = \exp(\mathrm{i}\pi/4)$, $\alpha_2 = 1$, $z_1 = K' + 2K\mathrm{i}/9$, and $z_2 = 3K'/4 + K\mathrm{i}/3$, the corresponding spectral parameters are $\lambda(z_1) \approx -1.301\mathrm{i}$ and $\lambda(z_2) \approx -0.504 - 0.429\mathrm{i}$. Substituting these parameters into the formula yields

the elliptic-soliton-breather solution shown in Fig. 4(b), with a maximum peak value of approximately 3.230. When $\alpha_1 = \alpha_2 = 1$, $z_1 = 0.176K' + 0.85K\mathrm{i}$, and $z_2 = 0.874K' + 0.174K\mathrm{i}$, the corresponding spectral parameters are $\lambda(z_1) \approx -0.945 - 0.591\mathrm{i}$ and $\lambda(z_2) \approx -0.874 - 0.895\mathrm{i}$. Substituting these parameters into the formula yields the elliptic-two-breather solution shown in Fig. 4(c), with a maximum peak value of approximately 3.397.

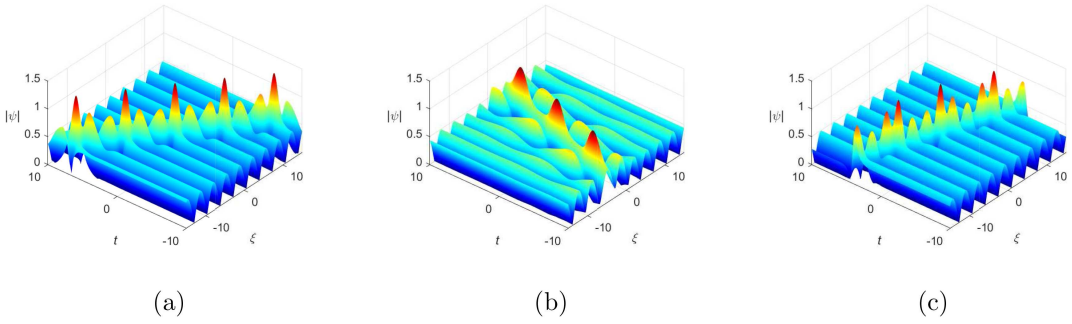


Fig. 3. Elliptic-breather solutions of the cmKdV equation on the cn-type background. (a) $\alpha_1 = 1$ and $z_1 = 3K'/4 + K\mathrm{i}/3$; (b) $\alpha_1 = 1$ and $z_1 = 0.5571 + 0.6743\mathrm{i}$; (c) $\alpha_1 = 1 + 0.5\mathrm{i}$ and $z_1 = 3K'/4 + K\mathrm{i}/4$.

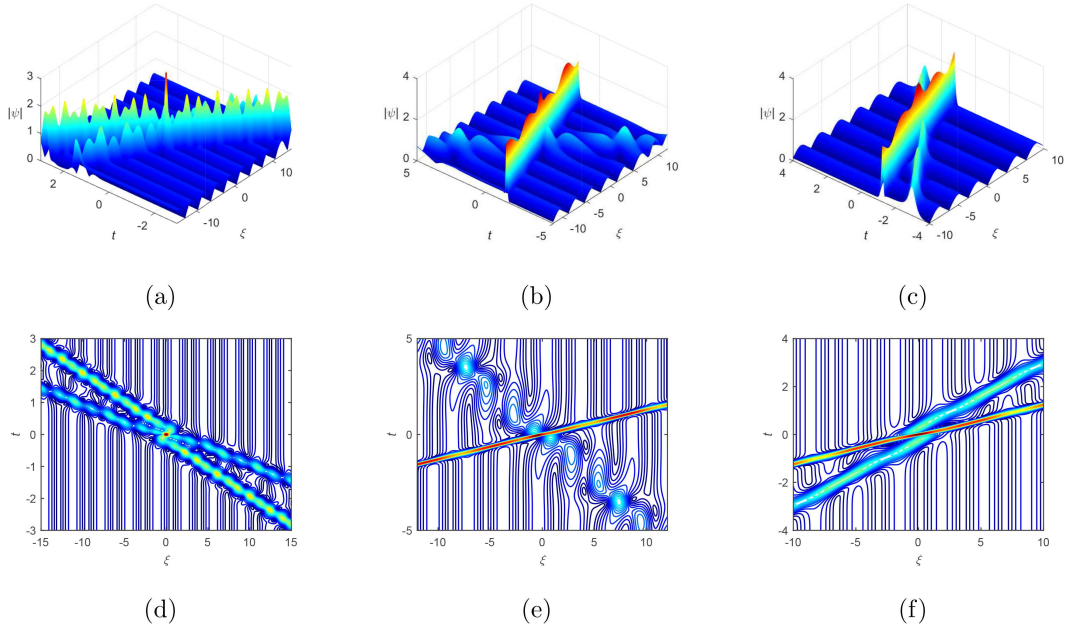


Fig. 4. Elliptic localized wave solutions on the cn-type background. (a)–(c) 3D plots of the elliptic-two-soliton, elliptic-soliton-breather, and elliptic-two-breather solutions, respectively. (d)–(f) Corresponding contour plots.

3.2. Dynamics of elliptic-localized wave solutions on dn-type backgrounds

In this subsection, setting the parameter $l = K'/2$ in Eq. (54), we obtain the dynamical characteristics of soliton and breather solutions on the dn-type background. Using the parameters $\alpha = 1$ and $k = 9/10$, we obtain $v_1 = 0$, $v_2 = -0.19$, $v_3 = 1$, and $s_2 = -0.595$.

When $\alpha_1 = 1$ and $z_1 = -K'/2 + K\mathrm{i}/5$, $\lambda(z_1) \approx -1.189\mathrm{i}$. Substituting these parameters into the Darboux transformation yields the elliptic-soliton solution shown in Fig. 5(a), where the soliton solution reaches a maximum value of approximately 3.3779 at the origin. When $\alpha_1 = 1 + 0.5\mathrm{i}$ and $z_1 = -K'/2 + 2K\mathrm{i}/5$, $\lambda(z_1) \approx -0.752\mathrm{i}$. Substituting these parameters into the Darboux transformation yields the elliptic-soliton solution shown in Fig. 5(b), where the maximum value of the soliton is approximately 1.5467. Although the spectral parameter still lies on the imaginary axis, the modulus of the free parameter $\alpha_1 = 1 + 0.5\mathrm{i}$ is $|\alpha_1| \approx 1.118 > 1$, which not only endows the solution with a complex phase structure but also introduces distinct asymmetric modulation features, causing the amplitude envelope of the soliton to exhibit a biased and asymmetric profile on the periodic background.

When $\alpha_1 = 1$, $z_1 = -K'/8 + 2K\mathrm{i}/5$, and $\lambda(z_1) \approx 0.103 - 0.535\mathrm{i}$, we obtain the elliptic-breather solution shown in Fig. 5(a), with a maximum peak value of approximately 2.070. When $\alpha_1 = 1$, $z_1 = -K'/5 + K\mathrm{i}/3$, and $\lambda(z_1) \approx 0.186 - 0.604\mathrm{i}$, we obtain the elliptic-breather solution shown in Fig. 6(b), where the maximum value of the breather is approximately 2.208. Due to the increase in the real part of z_1, the generated breather moves faster, exhibiting a distinctly inclined propagation path on the spatiotemporal plane

and demonstrating the dynamic translational characteristics of nonlinear waves for the cmKdV equation on an elliptic background. When $\alpha_1 = 1+0.5\mathrm{i}$, $z_1 = -K'/6+K\mathrm{i}/4$, and $\lambda(z_1) \approx 0.322-0.557\mathrm{i}$, we obtain the elliptic-breather solution shown in Fig. 6(c), where the maximum value of the solution is approximately 2.100. The introduction of the complex-valued free parameter $\alpha_1 = 1+0.5\mathrm{i}$ injects additional initial phase modulation into the breather, directly altering the symmetry and amplitude profile of the waveform and causing the breather's modulation on the periodic background to exhibit an asymmetric profile.

Next, setting the parameters $l = K'/2$ and $n = 2$ in Eq. (54), we obtain the elliptic-double-localized wave solutions on the dn-type background.

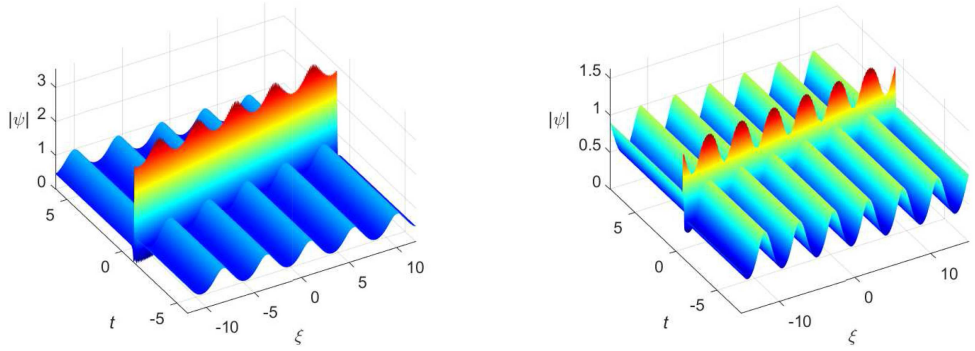


Fig. 5. Elliptic-soliton solutions of the cmKdV equation on the dn-type background. (a) $\alpha_1 = 1$ and $z_1 = -K'/2+K\mathrm{i}/5$; (b) $\alpha_1 = 1+0.5\mathrm{i}$ and $z_1 = -K'/2+2K\mathrm{i}/5$.

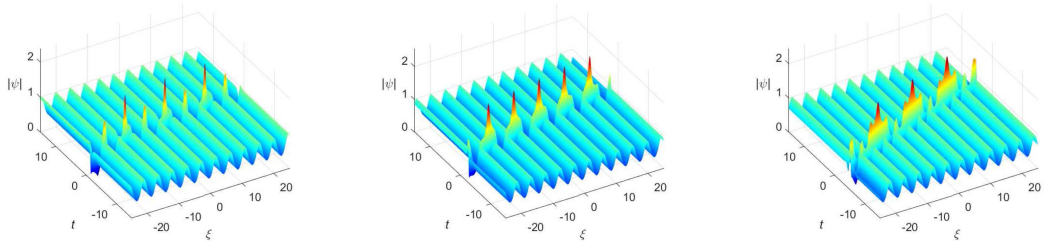


Fig. 6. Elliptic-breather solutions of the cmKdV equation on the dn-type background. (a) $\alpha_1 = 1$, $z_1 = -K'/8+2K\mathrm{i}/5$; (b) $\alpha_1 = 1$, $z_1 = -K'/5+K\mathrm{i}/3$; (c) $\alpha_1 = 1+0.5\mathrm{i}$, $z_1 = -K'/6+K\mathrm{i}/4$.

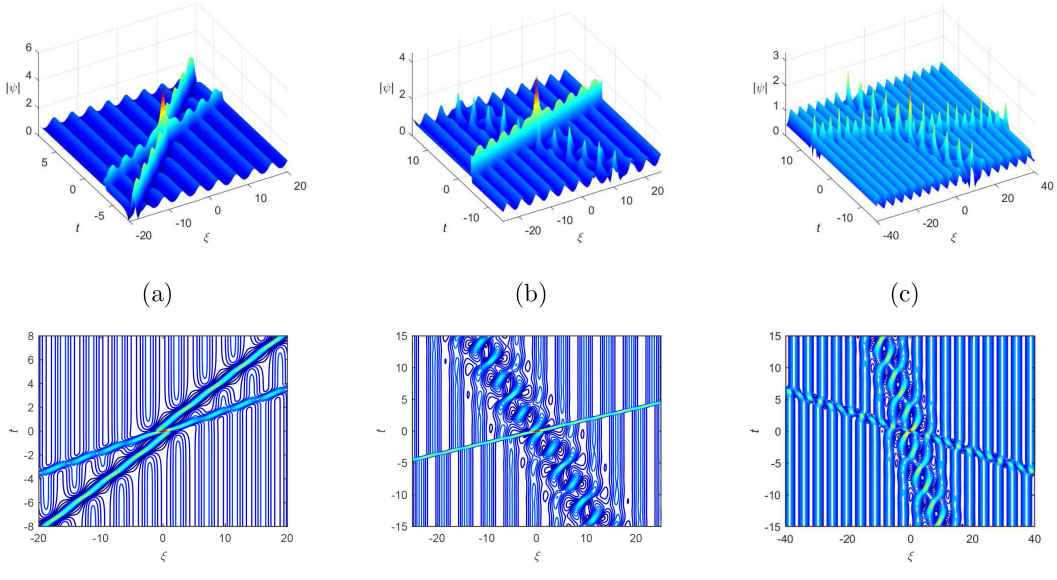


Fig. 7. Elliptic localized wave solutions on the dn-type background. (a)–(c) 3D plots of the elliptic-two-soliton, elliptic-soliton-breather, and elliptic-two-breather solutions, respectively. (d)–(f) Corresponding contour plots.

When $\alpha_1=\alpha_2=1$, $z_1=-K'/2+K\mathrm{i}/5$ and $z_2=-K'/2+2K\mathrm{i}/3$, the corresponding spectral parameters are $\lambda(z_1)\approx -1.189\mathrm{i}$ and $\lambda(z_2)\approx -0.821\mathrm{i}$. Substituting these parameters into the formula yields the elliptic-two-soliton solution shown in Fig. 7(a), with a maximum peak value of approximately 4.844. Taking $z_1=-K'/2+K\mathrm{i}/5$ and $z_2=-K'/5+K\mathrm{i}/3$, the corresponding spectral parameters are $\lambda(z_1)\approx -1.189\mathrm{i}$ and $\lambda(z_2)\approx 0.186-0.604\mathrm{i}$. Substituting these parameters into the formula yields the elliptic-soliton-breather solution shown in Fig. 7(b), with a maximum peak value of approximately 4.304. Taking $z_1=-K'/5+3K\mathrm{i}/20$ and $z_2=-K'/5+K\mathrm{i}/3$, the corresponding spectral parameters are $\lambda(z_1)\approx 0.584-0.534\mathrm{i}$ and $\lambda(z_2)\approx 0.186-0.604\mathrm{i}$. Substituting these parameters into the formula yields the elliptic-two-breather solution shown in Fig. 7(c), with a maximum peak value of approximately 3.151. From the corresponding contour plots, it can be observed that the two breather trajectories propagate on the dn-type periodic background at distinctly different velocities and inclination angles, each exhibiting a periodically expanding and contracting wave-like structure accompanied by closed vortex-like contour clusters. The two trajectories generate complex interference patterns in the intersection region and both recover their regular oscillation modes away from the collision area.

4. Elliptic rogue wave solutions

In this section, we utilize limit expansion techniques to address the degeneracy problem at the branch points. Specifically, by performing a small-parameter expansion of the spectral parameter near the branch points, we extract a second set of linearly independent solutions from the degenerate vector solutions.

Since the representation of the Theta function contains the parameters of the Abel map, we still use the original parameters to derive the formula for the rogue wave solutions. Assuming that we expand the eigenvalue λ_i around the branch point λ_1, we set $\lambda=\lambda_1+\varepsilon_1^2$, where ε_1 is a small parameter. We then obtain

$$y(\lambda)=\sqrt{(\lambda-\lambda_1)(\lambda-\lambda_2)(\lambda-\lambda_3)(\lambda-\lambda_4)}=\varepsilon_1 y_1 Y_1, \quad (58)$$

where

$$y_1=\sqrt{(\lambda_1-\lambda_2)(\lambda_1-\lambda_3)(\lambda_1-\lambda_4)},$$
$$Y_1=\sqrt{\left(1+\frac{\varepsilon_1^2}{\lambda_1-\lambda_2}\right)\left(1+\frac{\varepsilon_1^2}{\lambda_1-\lambda_3}\right)\left(1+\frac{\varepsilon_1^2}{\lambda_1-\lambda_4}\right)}.$$

Expanding the components in Eq. (49), we obtain

$$\begin{aligned}\beta_1(\lambda) &= 2(\lambda_1+\varepsilon_1^2)^2+s_2-2y(\lambda)\\ &= 2\lambda_1^2+s_2+2\varepsilon_1^2(2\lambda_1+\varepsilon_1^2)-2\varepsilon_1 y_1 Y_1,\\ C_1(\lambda) &= 2(\lambda_1+\varepsilon_1^2)(2\lambda_1^2+s_2+2\varepsilon_1^2(2\lambda_1+\varepsilon_1^2)\\ &\quad -2\varepsilon_1 y_1 Y_1)-s_3\\ &= 4\lambda_1^3+2s_2\lambda_1+4\big[\varepsilon_1^2(3\lambda_1^2+s_2/2+2\lambda_1\varepsilon_1^2+\varepsilon_1^4)\\ &\quad -\varepsilon_1 y_1 Y_1(\lambda_1+\varepsilon_1^2)\big]-s_3,\\ v(\tilde{\zeta})-\beta_1(\lambda) &= u_1(\tilde{\zeta})-2\varepsilon_1^2(\lambda_1+\varepsilon_1^2)+2\varepsilon_1 y_1 Y_1,\end{aligned}$$

where $u_1(\xi)=v(\xi)-(2\lambda_1^2+s_2)$. Substituting the above equations into the vector solution Φ_1 and expanding it into a Taylor series with respect to the small parameter ε_1, we obtain the required Taylor expansion coefficients. First, expanding the first component ϕ_1 into a Taylor series with a radius of convergence of 1, we have

$$\begin{aligned}\phi_1 &= \sqrt{v(\xi)-\beta_1(\lambda)}\exp(\theta_1)=\sum_{i=0}^{\infty}\phi_1^{[i]}\varepsilon_1^i,\\ \phi_1^{[i]} &= \frac{1}{i!}\frac{\partial^i\phi_1}{\partial\varepsilon_1^i}\bigg|_{\varepsilon_1=0},\\ \theta_1(\lambda) &= \mathrm{i}\int_0^{\xi}\frac{C_1}{v(s)-\beta_1}\mathrm{d}s+\mathrm{i}(\lambda_1+\varepsilon_1^2)\xi\\ &\quad +4\mathrm{i}\varepsilon_1 y_1 Y(\lambda_1+\varepsilon_1^2)-2\mathrm{i}s_3 t. \end{aligned} \quad (59)$$

From this, we can calculate the second component $\varphi_1=r_1\phi_1$ in the vector solution Φ_1. First, we need to derive the expression for r_1. From Eqs. (21) and (23), we obtain

$$\begin{aligned}r_1 &= \frac{m}{\mathrm{i}q-y}=\frac{2v(\xi)(\lambda_1-\varepsilon_1^2)-\mathrm{i}(v_\xi(\xi)/2+\mathrm{i}q)}{\mathrm{i}\sqrt{v(\xi)(v(\xi)-\beta_1(\lambda))}}\exp(-\theta_0),\\ \theta_0 &= \mathrm{i}s_3\int_0^{\xi}\frac{\mathrm{d}s}{v(s)}+2\mathrm{i}s_3 t. \end{aligned} \quad (60)$$

Thus, the expression for φ_1 is

$$\begin{aligned}\varphi_1 &= r_1\phi_1=\frac{2v(\xi)(\lambda_1-\varepsilon_1^2)-\mathrm{i}(v_\xi(\xi)/2+\mathrm{i}q)}{\sqrt{v(\xi)}\sqrt{v(\xi)-\beta_1(\lambda)}}\exp(\theta_1-\theta_0)\\ &= \sum_{i=0}^{\infty}\varphi_1^{[i]}\varepsilon_1^i, \end{aligned} \quad (61)$$

where $\varphi_1^{[i]}=\frac{1}{i!}\frac{\partial^i\varphi_1}{\partial\varepsilon_1^i}\Big|_{\varepsilon_1=0}$.

Similarly, we choose another eigenvalue for the iteration to obtain a new solution. Taking λ_2, we set $\lambda=\lambda_2+\varepsilon_2^2$, where ε_2 is a small parameter. Following the expansion steps described above, we obtain the expressions for ϕ_2 and φ_2

$$\phi_2=\sum_{i=0}^{\infty}\phi_2^{[i]}\varepsilon_2^i, \quad \varphi_2=\sum_{i=0}^{\infty}\varphi_2^{[i]}\varepsilon_2^i, \quad (62)$$

where $\phi_2^{[i]}$ and $\varphi_2^{[i]}$ have the same forms as $\phi_1^{[i]}$ and $\varphi_1^{[i]}$, obtained simply by replacing λ_1 with λ_2.

Through the following integral formulas:

$$\begin{aligned}V_0 &= u, \quad V_1=\int\frac{\mathrm{d}u}{1-\alpha^2\,\mathrm{sn}^2 u}=\Pi(\varphi,\alpha^2,k), \quad \varphi=\mathrm{am}\,u,\\ V_2 &= \frac{1}{2(\alpha^2-1)(k^2-\alpha^2)}\Big[\alpha^2E(u)+(k^2-\alpha^2)u\\ &\quad +(2\alpha^2(1+k^2)-\alpha^4-3k^2)\eta_1-\frac{\alpha^4\,\mathrm{sn}\,u\,\mathrm{cn}\,u\,\mathrm{dn}\,u}{1-\alpha^2\,\mathrm{sn}^2 u}\Big]. \end{aligned} \quad (63)$$

Below, we take a few specific rogue waves as examples. First, we consider the first-order rogue wave. We give the expressions for $\phi_1^{[1]}$ and $\varphi_1^{[1]}$

$$\begin{aligned}\phi_1^{[1]} &= \sqrt{u_1(x)W_1}\exp(\theta_1(\xi,t)),\\ \theta_1(\xi,t) &= \mathrm{i}\int_0^{\xi}\frac{\mathrm{d}s}{v(s)}+\mathrm{i}\lambda_1\xi,\\ \varphi_1^{[1]} &= \sqrt{v(x)}\sqrt{u_1(x)}\frac{2-u_1(x)W_1}{W_2}\exp(\theta_1-\theta_0),\end{aligned}\tag{64}$$

where $W_1=\frac{1}{u_1(\xi)}-2\mathrm{i}\left(\int_0^{\xi}\frac{2\lambda_1}{u_1(s)}\mathrm{d}s-\int_0^{\xi}\frac{C_1(\lambda)}{u_1^2(\xi)}\mathrm{d}s\right)+4\mathrm{i}\lambda_1 t+o_1$, $W_2=2\lambda_1 v(\xi)+\mathrm{i}\frac{v'(\xi)}{2}$, $k_1\in\mathbb{C}$. Considering the singularity of W_1, we rewrite its expression using λ_i $(i=1,2,3,4)$ as

$$\begin{aligned}W_1 &= \frac{1}{u_1(\xi)}+4\mathrm{i}\lambda_1 t+o_1+Q_1\left(\frac{E}{K}\varepsilon\xi+Z(\varepsilon\xi)\right)+Q_2\xi\\ &\quad+Q_3\frac{\mathrm{sn}(\varepsilon\xi)\,\mathrm{cn}(\varepsilon\xi)\,\mathrm{dn}(\varepsilon\xi)}{u_1(\xi)},\end{aligned}\tag{65}$$

where $\varepsilon=\sqrt{4b^2+(c+d)^2}$, $Q_0=(\lambda_1-\lambda_2)(\lambda_1-\lambda_2^*)$, $Q_1=-\frac{\varepsilon}{2cQ_0}$, $Q_2=\frac{1}{2c}$, and $Q_3=\frac{2\varepsilon d}{Q_0}$.

Based on the above, we substitute $\left(\phi_1^{[1]},\varphi_1^{[1]}\right)^{\mathrm{T}}$ into the Darboux transformation and thereby obtain the first-order rogue wave solution on the periodic wave background

$$\psi_1 = \sqrt{v(\xi)}\left(1-\frac{8\mathrm{i}\,\mathrm{Im}(\lambda_1)W_2\left[\lambda_1^{*2}-(2\lambda_1^2-u_1(\xi))|W_1|^2/2+W_1\right]}{|W_2|^2|W_1|^2+v(\xi)\left|\lambda_1^2-(2\lambda_1^2+u_1(\xi))W_1/2+1\right|^2}\right)\exp(-\theta_0).\tag{66}$$

Furthermore, substituting $\Phi_1=(\phi_1^{[1]},\varphi_1^{[1]})^{\mathrm{T}}$ and $\Phi_2=(\phi_2^{[1]},\varphi_2^{[1]})^{\mathrm{T}}$ into the Darboux transformation, we obtain the second-order rogue wave solution on the periodic wave background

$$\psi_2=\sqrt{v(\xi)}\left[\frac{\det(\boldsymbol{K}_2)}{\det(\boldsymbol{U}_2)}\right]\exp(-\theta_0),\tag{67}$$

where

$$\boldsymbol{U}_2=\begin{bmatrix}\dfrac{|\varphi_1|^2+|\phi_1|^2}{\lambda_1-\lambda_1^*} & \dfrac{\phi_1^*\varphi_2+\phi_1^*\phi_2}{\lambda_2-\lambda_1^*}\\ \dfrac{\varphi_1\varphi_2^*+\phi_1\phi_2^*}{\lambda_1-\lambda_2^*} & \dfrac{|\varphi_2|^2+|\phi_2|^2}{\lambda_2-\lambda_2^*}\end{bmatrix},$$

$$\boldsymbol{K}_2=\boldsymbol{U}_2-\frac{2\mathrm{e}^{-\theta_0}}{\sqrt{v(\xi)}}\begin{bmatrix}\phi_1^*\phi_1 & \phi_1^*\phi_2\\ \phi_2^*\phi_1 & \phi_2^*\phi_2\end{bmatrix},$$

where ϕ_i and φ_i are given in Eqs. (59) and (61).

4.1. Dynamics of rogue wave solutions on the cn-type background

Since the cmKdV equation possesses scale symmetry, we can fix the amplitude of the background. Therefore, we select the parameters $c=d=0.5$, which yield $v_1=-4b^2$, $v_2=0$, $v_3=1$, $m=1/(1+4b^2)$, $s_2=1-2b^2$, and $q=-s_3=0$. Thus, the corresponding elliptic-function solution is

$$\psi=\mathrm{cn}\left(\sqrt{1+4b^2}\,\xi\,\middle|\,m\right)\mathrm{e}^{\theta_0}.$$

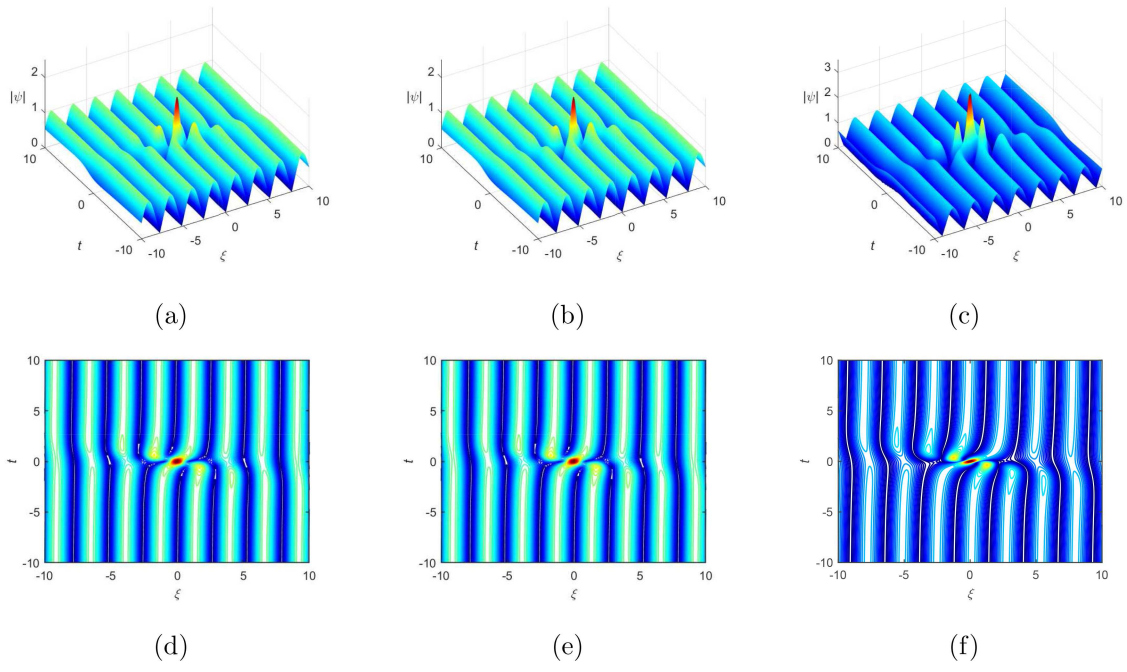


Fig. 8. Rogue wave solutions on the cn-type background. (a) 3D plot of the first-order rogue wave. (b) 3D plot of another first-order rogue wave. (c) 3D plot of the second-order rogue wave. (d)–(f) Corresponding contour plots.

By fixing the background solution, two distinct families of rogue wave solutions originating from two branch points can be obtained using Eq. (66). In this case, we find that the rogue waves corresponding to the two branch points are identical. Choosing the parameters $b = 0.5$, $\lambda_1 = 0.5 + 0.5\mathrm{i}$, and $o_1 = 0$, we plot the profile of the first-order rogue wave on the cn-type background, as shown in Fig. 8(a). Similarly, by changing the spectral parameter to $\lambda_2 = -0.5 + 0.5\mathrm{i}$, we obtain another first-order rogue wave profile on the cn-type background, as shown in Fig. 8(b). The two branch points are related by the involution symmetry $\lambda_2 = -\lambda_1^*$ of the Lax pair, producing solutions with the same modulus but different phases at the two locations. Hence, the profiles in Figs. 8(a) and 8(b) are completely identical.

For the second-order rogue wave, we set the parameters $b = 0.5$, $\lambda_1 = 0.5 + 0.5\mathrm{i}$, $\lambda_2 = -0.5 + 0.5\mathrm{i}$, and $o_1 = o_2 = 0$ to obtain the second-order rogue wave profile shown in Fig. 8(c), whose maximum value at the origin is 3. If we change the parameters o_1 and o_2, the position of the second-order rogue wave changes accordingly.

4.2. Dynamics of rational solutions on the dn-type background

Since the cmKdV equation possesses scale symmetry, we can fix the amplitude of the background. Therefore, we select the parameters $b = 0$, $c = \frac{1}{2}(1 + k_1)$, and $d = \frac{1}{2}(1 - k_1)$, where $k_1 \neq 1$. Then, $v_1 = 0$, $v_2 = -k_1^2$, $v_3 = 1$, $m = 1 - k_1^2$, $s_2 = \frac{1}{2}(1 - k_1^2)$, and $q = -s_3 = 0$. Thus, the corresponding elliptic-function solution is

$$\psi = \mathrm{dn}(\xi \mid m)\, \mathrm{e}^{\theta_0}.$$

Because the cmKdV equation is modulationally stable on the dn-type background, the solutions on the dn-type background, unlike the strict rogue waves that can be constructed on the cn-type background, do not possess the typical characteristics of rogue waves. Instead, they manifest as nonlinear superpositions of solitons or breathers with periodic waves.

Choosing the parameters $k_1 = 1/3$, $\lambda_1 = 2\mathrm{i}/3$, and $o_1 = 0$, and substituting them into Eq. (66), we obtain the elliptic-soliton solution on the dn-type background, as shown in Fig. 9(a), with a maximum value of $7/3$. This solution exhibits a nonlinear superposition of an algebraically decaying soliton and a dn periodic wave, propagating along a specific direction; the peak arrives from a distance and eventually departs. Away from the localized region, it still displays the characteristics of the dn solution. Choosing another set of parameters, $k_1 = 1/3$, $\lambda_1 = \mathrm{i}/3$, and $o_1 = 0$, we obtain the elliptic-breather solution on the dn-type background, as shown in Fig. 9(b). Its amplitude oscillates quasi-periodically in the temporal direction, while the perturbation propagates along the spatial direction without localized decay, attaining a maximum value of $5/3$ at the origin.

Choosing the parameters $k_1 = 1/3$, $\lambda_1 = 2\mathrm{i}/3$, $\lambda_2 = \mathrm{i}/3$, and $o_1 = o_2 = 0$, and substituting them into the second-order rogue wave Eq. (67), we obtain the elliptic-soliton-breather solution located at the origin, with a maximum value of 3, as shown in Fig. 9(c). This solution is accompanied by a quasi-periodically oscillating structure along the spatial periodic direction, which can be understood as the coupled nonlinear superposition of nonlinear modes corresponding to two different spectral parameters.

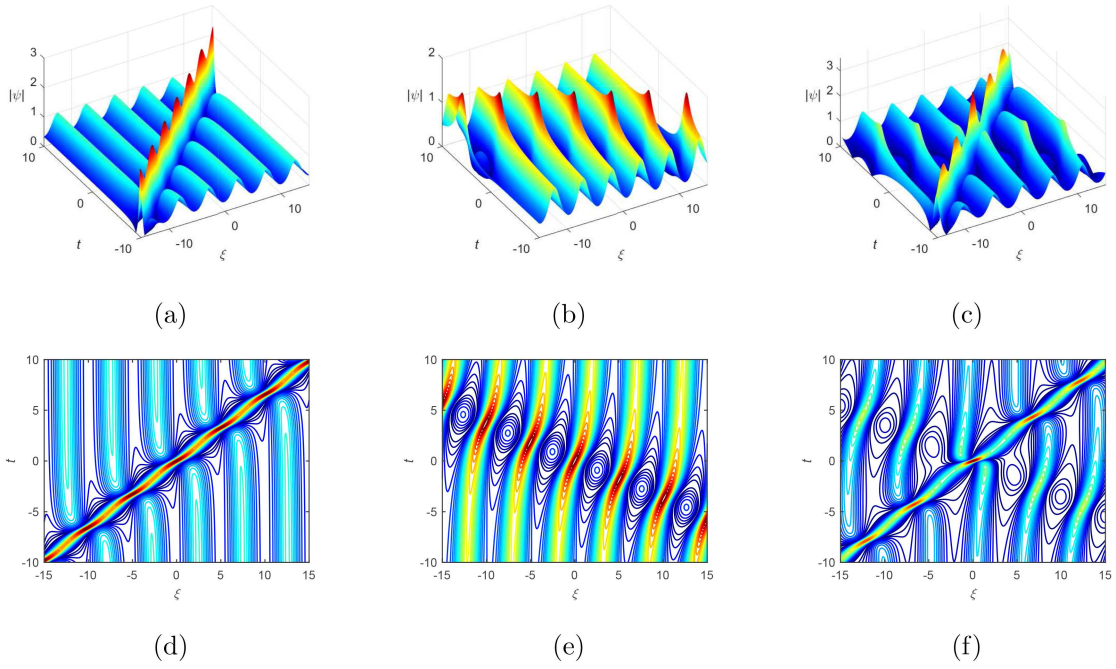


Fig. 9. Rational solutions on the dn-type background. (a) 3D plot of the elliptic-soliton solution with $\lambda_1 = 2\mathrm{i}/3$. (b) 3D plot of the elliptic-breather solution with $\lambda_1 = \mathrm{i}/3$. (c) 3D plot of the elliptic-soliton-breather solution. (d)–(f) Corresponding contour plots of the solutions in (a)–(c).

5. Conclusion

This paper systematically investigates the localized wave solutions and rogue wave solutions of the cmKdV equation on elliptic-function backgrounds by combining the Theta function representation with the Darboux transformation. Within the genus-1 framework, complete Theta function representations for the elliptic-function periodic solutions and the fundamental solutions of the Lax pair are derived. Utilizing linear combinations of the vector solutions of the Lax pair and the Theta function addition formula, explicit determinant formulas for the n-th-order localized wave solutions are established. Furthermore, five types of localized waves—elliptic-solitons, elliptic-breathers, elliptic-two-solitons, elliptic-soliton-breathers, and elliptic-two-breathers—are constructed on the cn-type and dn-type backgrounds. By means of small-parameter expansions at the branch points of the spectral curve, general determinant formulas for the n-th-order rogue waves are derived. It is revealed that on the cn-type background, two identical rogue waves are obtained due to the relation $\lambda_2 = -\lambda_1^*$, and the coexistence of different families of rogue waves is verified through the second-order rogue waves. On the dn-type background, owing to its modulational stability, two distinct branch points generate elliptic-solitons and elliptic-breathers, respectively, which manifest as elliptic-soliton-breather solutions in the second-order case.

Future work can be developed along the following aspects: the regulatory effects of the free parameters o_i on the splitting configurations of higher-order rogue waves remain to be systematically revealed; generalizing the background from genus 1 to the hyperelliptic cases of genus $g \geq 2$ is a challenging direction; the technical approach developed in this paper is expected to be extended to other integrable systems, such as the Sasa–Satsuma equation; furthermore, numerical verification of the robustness of these solutions and exploration of their experimental observability in ultrashort pulse transmission are also important research directions.

Appendix A: Darboux transformation on the elliptic-function backgrounds

In this appendix, we present the relevant results on the Darboux transformation. The theory of Darboux transformations is well established. The classical Darboux transformation, the n-fold Darboux transformation, and the generalized Darboux transformation are described by the following theorems, which form the foundation for constructing multi-fold and higher-order solutions.

Theorem A1 Suppose that for the Lax pair (2), there exists an entire matrix function $\Phi(x,t,\lambda)$ in λ. Its potential function satisfies $\psi(x,t) \in L^\infty(\mathbb{R}^2) \cap C^\infty(\mathbb{R}^2)$, and at $(x,t) = (0,0)$ the normalization $\Phi(0,0;\lambda) = \mathbb{I}$ holds. Then the Darboux transformation is given by

$$T_1(x,t,\lambda) = \mathbb{I} - \frac{\lambda_1 - \lambda_1^*}{\lambda - \lambda_1^*} P_1, \quad P_1 = \frac{\Phi_1 \Phi_1^\dagger}{\Phi_1^\dagger \Phi_1}, \tag{A1}$$

where $\Phi_1 = \Phi(x,t;\lambda_1)(1, c_1)^{\mathrm{T}} \equiv (\phi_1, \varphi_1)^{\mathrm{T}}$ is a particular solution at $\lambda = \lambda_1$. This transformation maps the Lax pair (2) into a new system of the same form, with the new potential function

$$\psi_1(x,t) = \psi(x,t) + \frac{2(\lambda_1^* - \lambda_1)\,\varphi_1^* \phi_1}{|\phi_1|^2 + |\varphi_1|^2}, \tag{A2}$$

and the normalized fundamental matrix solution of the new system is $\Phi[1] = T_1(x,t,\lambda)\,\Phi(x,t,\lambda)\,T_1(0,0;\lambda)^{-1}$, which is also an entire matrix function in λ. By iterating the classical Darboux transformation, one can systematically construct the n-fold Darboux transformation matrix. The n-fold Darboux transformation is a purely algebraic iterative procedure. Selecting n mutually distinct spectral parameters λ_i $(i = 1,2,\ldots,n)$ and their corresponding eigenvectors $\Phi_i = \Phi(x,t;\lambda_i)(1, c_i)^{\mathrm{T}}$, the n-fold iteration can be compactly written as the n-fold Darboux matrix

$$\boldsymbol{T}[n](x,t,\lambda) = \mathbb{I} - \boldsymbol{X}_n(x,t)\,\boldsymbol{U}_n(x,t)^{-1}\,\boldsymbol{L}_n(\lambda)^{-1}\,\boldsymbol{X}_n(x,t)^\dagger, \tag{A3}$$

where

$$\boldsymbol{D}_n(x,t) = \left(\frac{\Phi_i^\dagger \Phi_j}{\lambda_j - \lambda_i^*}\right)_{1 \leq i,j \leq n},$$
$$\boldsymbol{X}_n(x,t) = [\Phi_1, \Phi_2, \ldots, \Phi_n],$$
$$\boldsymbol{L}_n(\lambda) = \mathrm{diag}(\lambda - \lambda_1, \ldots, \lambda - \lambda_n).$$

The corresponding n-fold Bäcklund transformation formula[48] is

$$\psi_n = \psi - 2\boldsymbol{X}_{n,1}\,\boldsymbol{U}_n(x,t)^{-1}\,\boldsymbol{X}_{n,2}^\dagger. \tag{A4}$$

Generalized Darboux transformation: When the iteration is performed at identical spectral parameters, the spectral point becomes a movable singularity, necessitating a limiting procedure combined with a Taylor expansion mechanism. For the two pairs of conjugate branch points on the elliptic background, we expand at λ_1 and λ_2

$$\Phi(x,t,\lambda) = \sum_{i=0}^{\infty} \Phi_a^{[i]} (\lambda - \lambda_a)^i, \quad a = 1,2.$$

Using the expansion coefficients, one can construct the generalized Darboux matrix

$$\boldsymbol{T}[n_1,n_2](x,t,\lambda) = \mathbb{I} - \boldsymbol{X}\boldsymbol{U}^{-1}\boldsymbol{D}\boldsymbol{X}^\dagger, \;\; \boldsymbol{M} = \boldsymbol{Y}\boldsymbol{V}\boldsymbol{Y}^\dagger, \tag{A5}$$

where the block matrix elements are defined as

$$\boldsymbol{V}_{a,b} = \left(\frac{(-1)^{j+1}}{(\lambda_b - \lambda_a^*)^{i+j+1}} \binom{i+j-2}{i-1}\right)_{1 \leq i \leq n_a, 1 \leq j \leq n_b},$$
$$\boldsymbol{X} = [\boldsymbol{X}_1, \boldsymbol{X}_2], \quad \boldsymbol{Y} = \mathrm{diag}(\boldsymbol{Y}_1, \boldsymbol{Y}_2),$$

$$\boldsymbol{L} = \mathrm{diag}(\boldsymbol{L}_1, \boldsymbol{L}_2),$$

where $\boldsymbol{X}_a$, $\boldsymbol{Y}_a$, and $\boldsymbol{D}_a$ are constructed from the derivative coefficients $\boldsymbol{\Phi}_a^{[i]}$ arranged in lower-triangular or anti-diagonal patterns. The resulting higher-order Bäcklund transformation is

$$\psi_{n_1,n_2} = \psi - 2\boldsymbol{X}_1 \boldsymbol{U}^{-1} \boldsymbol{X}_2^{\dagger}. \tag{A6}$$

Appendix B: Elliptic functions and related formulas

Definition B1 Jacobi elliptic functions[57] Based on the elliptic integral of the first kind, we introduce the integral relation in terms of the parameters y and k

$$\begin{aligned} u(y,k) &= \int_0^y \frac{\mathrm{d}t}{\sqrt{(1-t^2)(1-k^2t^2)}} \\ &= \int_0^u \frac{\mathrm{d}\theta}{\sqrt{1-k^2\sin^2\theta}}. \end{aligned} \tag{B1}$$

The inverse function of this integral relation is defined as the Jacobi elliptic sine function sn, written as $y = \mathrm{sn}(u)$.

Definition B2 Theta functions[57] The Theta function can be defined by the following series:

$$\vartheta_{a,b}(u|\tau) := \sum_{n\in\mathbb{Z}} \mathrm{e}^{\mathrm{i}\pi\tau(n+a)^2+2\pi\mathrm{i}(n+a)(u+b)}, \tag{B2}$$

and

$$\begin{aligned} &\vartheta_1(u|\tau) = -\vartheta_{\frac{1}{2},\frac{1}{2}}(u|\tau), \quad \vartheta_2(u|\tau) = \vartheta_{\frac{1}{2},0}(u|\tau), \\ &\vartheta_3(u|\tau) = \vartheta_{0,0}(u|\tau), \quad \vartheta_4(u|\tau) = \vartheta_{0,\frac{1}{2}}(u|\tau). \end{aligned} \tag{B3}$$

We may also write $\vartheta_j(u,q) = \vartheta_j(u|\tau)$, where the nome $q = \mathrm{e}^{\mathrm{i}\pi\tau}$, $\tau = \mathrm{i}K'/K$, $K = K(m)$, and $K' = K(1-m)$. The shorthand $\vartheta_j = \vartheta_j(0|\tau)$ is frequently used. The Jacobi elliptic functions expressed in terms of Theta functions are

$$\begin{aligned} &\mathrm{sn}(2Ku) = \frac{\vartheta_3}{\vartheta_2}\frac{\vartheta_1(u)}{\vartheta_4(u)}, \quad \mathrm{cn}(2Ku) = \frac{\vartheta_4}{\vartheta_2}\frac{\vartheta_2(u)}{\vartheta_4(u)}, \\ &\mathrm{dn}(2Ku) = \frac{\vartheta_4}{\vartheta_3}\frac{\vartheta_3(u)}{\vartheta_4(u)}. \end{aligned} \tag{B4}$$

The elliptic parameters are given by $m = \vartheta_2^4/\vartheta_3^4$ and $m' = 1-m = \vartheta_4^4/\vartheta_3^4$. We introduce the Jacobi zeta function

$$Z(u|m) = \frac{1}{2K}\frac{\vartheta_4'\left(\frac{u}{2K}\right)}{\vartheta_4\left(\frac{u}{2K}\right)} = \frac{\mathrm{d}}{\mathrm{d}u}\ln\vartheta_4\left(\frac{u}{2K}\right). \tag{B5}$$

The three-term Weierstrass addition formulas are given by

$$\begin{aligned} &\vartheta_1(a+b)\,\vartheta_2(a-b)\,\vartheta_3(c+d)\,\vartheta_4(c-d) \\ &-\vartheta_1(a-c)\,\vartheta_2(a+c)\,\vartheta_3(c-b)\,\vartheta_4(c+b) \\ =\ &\vartheta_1(b+d)\,\vartheta_2(b-d)\,\vartheta_3(a+c)\,\vartheta_4(a-c), \\ &\vartheta_1(u+a)\,\vartheta_1(u-a)\,\vartheta_4(v+b)\,\vartheta_4(v-b) \\ &-\vartheta_1(v+a)\,\vartheta_1(v-a)\,\vartheta_4(u+b)\,\vartheta_4(u-b) \\ =\ &\vartheta_1(u+v)\,\vartheta_1(u-v)\,\vartheta_4(a+b)\,\vartheta_4(a-b), \\ &\vartheta_2(u+a)\,\vartheta_2(u-a)\,\vartheta_4(v+b)\,\vartheta_4(v-b) \\ &+\vartheta_1(u+v)\,\vartheta_1(u-v)\,\vartheta_3(a+b)\,\vartheta_3(a-b) \\ =\ &\vartheta_2(v+a)\,\vartheta_2(v-a)\,\vartheta_4(u+b)\,\vartheta_4(u-b), \\ &\vartheta_2(u+v)\,\vartheta_2(u-v)\,\vartheta_2(a+b)\,\vartheta_2(a-b) \\ &-\vartheta_3(u+a)\,\vartheta_3(u-a)\,\vartheta_3(v+b)\,\vartheta_3(v-b) \\ =\ &-\vartheta_4(v+a)\,\vartheta_4(v-a)\,\vartheta_4(u+b)\,\vartheta_4(u-b). \end{aligned} \tag{B6}$$

The half-period translation formulas are standard identities for shifting Theta function arguments by half-periods and are used throughout the main text

$$\begin{aligned} \vartheta_1\left(u+\frac{1+\tau}{2}\right) &= \mathrm{e}^{-\pi\mathrm{i}(u+\tau/4)}\vartheta_3(u), \\ \vartheta_2\left(u+\frac{1+\tau}{2}\right) &= -\mathrm{i}\,\mathrm{e}^{-\pi\mathrm{i}(u+\tau/4)}\vartheta_4(u), \\ \vartheta_3\left(u+\frac{1+\tau}{2}\right) &= \mathrm{i}\,\mathrm{e}^{-\pi\mathrm{i}(u+\tau/4)}\vartheta_1(u), \\ \vartheta_4\left(u+\frac{1+\tau}{2}\right) &= \mathrm{e}^{-\pi\mathrm{i}(u+\tau/4)}\vartheta_2(u). \end{aligned} \tag{B7}$$

Acknowledgment

This work was supported by the National Natural Science Foundation of China (Grant No. 12575004).

References

[1] Zabusky N J and Kruskal M D 1965 *Phys. Rev. Lett.* **15** 240
[2] Gardner C S, Greene J M, Kruskal M D and Miura R M 1967 *Phys. Rev. Lett.* **19** 1095
[3] Lax P D 1968 *Commun. Pure Appl. Math.* **21** 467
[4] Liu W, Dao L and Zhang R 2025 *Chin. Phys. B* **34** 070504
[5] Shabat A and Zakharov V 1972 *Sov. Phys. JETP* **34** 62
[6] Ablowitz M J, Kaup D J, Newell A C and Segur H 1973 *Phys. Rev. Lett.* **31** 125
[7] Ablowitz M J, Kaup D J, Newell A C and Segur H 1974 *Stud. Appl. Math.* **53** 249
[8] Wadati M 1972 *J. Phys. Soc. Jpn.* **32** 1681
[9] Wadati M 1973 *J. Phys. Soc. Jpn.* **34** 1289
[10] Leblond H, Triki H, Sanchez F and Mihalache D 2012 *Opt. Commun.* **285** 356
[11] Leblond H and Mihalache D 2009 *Phys. Rev. A* **79** 063835
[12] Leblond H and Mihalache D 2013 *Phys. Rep.* **523** 61
[13] He J, Wang L, Li L, Porsezian K and Erdélyi R 2014 *Phys. Rev. E* **89** 062917
[14] Lan Z Z 2024 *Chin. Phys. B* **33** 060201
[15] Gorbacheva O B and Ostrovsky L A 1983 *Physica D* **8** 223
[16] Miura R M, Gardner C S and Kruskal M D 1968 *J. Math. Phys.* **9** 1204
[17] Magri F 1978 *J. Math. Phys.* **19** 1156
[18] Hirota R 1971 *Phys. Rev. Lett.* **27** 1192
[19] Hirota R 1972 *J. Phys. Soc. Jpn.* **33** 1456
[20] Matveev V B and Salle M A 1991 *Darboux Transformations and Solitons* (Berlin: Springer)
[21] Gu C, Hu H and Zhou Z 2004 *Darboux Transformations in Integrable Systems: Theory and Their Applications to Geometry* (Dordrecht: Springer Science & Business Media)

[22] Rogers C and Shadwick W F 1982 *Bäcklund Transformations and Their Applications* (New York: Academic Press)
[23] Its A 2003 *Not. Am. Math. Soc.* **50** 1389
[24] Novikov S, Manakov S V, Pitaevskii L P and Zakharov V E 1984 *Theory of Solitons: The Inverse Scattering Method* (New York: Springer)
[25] Faddeev L D and Takhtajan L A 1987 *Hamiltonian Methods in the Theory of Solitons* (Berlin: Springer)
[26] Guo B, Ling L and Liu Q P 2012 *Phys. Rev. E* **85** 026607
[27] Guo B, Ling L and Liu Q P 2013 *Stud. Appl. Math.* **130** 317
[28] Xu S, He J and Wang L 2011 *J. Phys. A: Math. Theor.* **44** 305203
[29] Tao Y and He J 2012 *Phys. Rev. E* **85** 026601
[30] He J S, Zhang H R, Wang L H, Porsezian K and Fokas A S 2013 *Phys. Rev. E* **87** 052914
[31] Yang B and Yang J 2024 *Rogue Waves in Integrable Systems* (Cham: Springer Nature)
[32] Wadati M and Ohkuma K 1982 *J. Phys. Soc. Jpn.* **51** 2029
[33] Tsuchida T and Wadati M 1998 *J. Phys. Soc. Jpn.* **67** 1175
[34] Alejo M A and Muñoz C 2013 *Commun. Math. Phys.* **324** 233
[35] Alejo M and Muñoz C 2015 *Anal. PDE* **8** 629
[36] Novikov S P 1974 *Funct. Anal. Its Appl.* **8** 236
[37] Dubrovin B A, Matveev V B and Novikov S P 1976 *Russ. Math. Surv.* **31** 59
[38] Belokolos E D 1994 *Algebro-Geometric Approach to Nonlinear Integrable Equations* (Berlin: Springer)
[39] Cao C, Wu Y and Geng X 1999 *J. Math. Phys.* **40** 3948
[40] Chen J and Pelinovsky D E 2018 *Proc. R. Soc. A* **474** 20170814
[41] Ling L and Sun X 2024 *Phys. Rev. E* **109** 064209
[42] Xu G, Chabchoub A, Pelinovsky D E and Kibler B 2020 *Phys. Rev. Res.* **2** 033528
[43] Chen J, Pelinovsky D E and White R E 2019 *Phys. Rev. E* **100** 052219
[44] Chen J, Pelinovsky D E and White R E 2020 *Physica D* **405** 132378
[45] Grinevich P G and Santini P M 2018 *Nonlinearity* **31** 5258
[46] Bertola M, El G A and Tovbis A 2016 *Proc. R. Soc. A* **472** 20160340
[47] Bertola M and Tovbis A 2017 *Commun. Math. Phys.* **354** 525
[48] Feng B F, Ling L and Takahashi D A 2020 *Stud. Appl. Math.* **144** 46
[49] Chen J and Pelinovsky D E 2018 *Nonlinearity* **31** 1955
[50] Chen J and Pelinovsky D E 2019 *J. Nonlinear Sci.* **29** 2797
[51] Ling L and Sun X 2023 *Adv. Math.* **435** 109356
[52] Ling L and Sun X 2023 *Stud. Appl. Math.* **150** 135
[53] Sinthuja N, Manikandan K and Senthilvelan M 2021 *Phys. Scr.* **96** 105206
[54] Rao J, Mihalache D and He J 2025 *Appl. Math. Lett.* **160** 109308
[55] Hu W and Gegen H 2025 *Chin. Phys. B* **34** 070202
[56] Kamchatnov A M 1997 *Phys. Rep.* **286** 199
[57] Byrd P F and Friedman M D 2013 *Handbook of Elliptic Integrals for Engineers and Physicists* (Berlin: Springer)